Natural frequency assignment of a pipeline through structural modification in layout optimization of elastic supports

Lin Zhang[a], Tao Zhang[a,*], Huajiang Ouyang[b], Tianyun Li[a], Mo You[c]

[a] *School of Naval Architecture & Ocean Engineering, Huazhong University of Science and Technology Wuhan, Hubei 430074, China*

[b] *School of Engineering, University of Liverpool, Liverpool L69 3GH, U.K.*

[c] *China Ship Development and Design Center, Wuhan, Hubei 430064, China*

Abstract: Layout optimization of elastic supports is an effective approach to address the resonance problem of an industrial post-manufactured pipeline. However, previous investigations of support layout optimization of a post-manufactured pipeline usually require establishing or updating the numerical model of the whole pipeline system, which may lead to time-consuming calculations and poor optimization results. In order to overcome these drawbacks, a new measurement-based layout optimization method is proposed in this method. Only a small number of experimental modal parameters (natural frequencies, damping ratios, and mode shapes) are needed in this method. Resonance avoidance, in this method, is recast as an assignment of natural frequencies, and the target natural frequencies are realized by performing structural modification in two stages. In addition, each of the elastic supports is viewed as a mass-spring-damper sub-system in this paper, which is represented by its measured dynamic stiffness and does not need a pre-determined simplified form. A numerical example demonstrates that the proposed method can accurately realize the target natural frequencies. The application of the proposed method to optimize the support layout of a real L-shaped pipeline system provides experimental evidence of its effectiveness. This experiment is the first attempt to achieve the layout optimization of pipeline supports for solving the resonance problem of a post-manufacture pipeline, entirely relying on the measured modal data.

Keywords: Post-manufactured pipeline; natural frequency assignment; layout optimization; structural modification.

1. Introduction

A pipeline system is commonly employed to connect power and energy supply equipment and mass transport equipment and thus plays a crucial role in the engineering field [1-3]. However, an industrial pipeline system often undergoes excessive vibration, potentially compromising pipeline function and safety [4-6]. One reason for such problems is resonance, which is caused by excitation whose frequency is close to a natural frequency of a pipeline system [7,8]. Resonance is dangerous since it can cause large structural deformations, leading to fatigue or even catastrophic structural failure [9,10]. Therefore, it is crucial to suppress the resonance problem of industrial pipeline systems.

Conventionally, shifting a natural frequency of a pipeline away from the frequency of excitation by parameter optimization is an effective way to solve the resonance problem of a pipeline system [11]. However, the material and geometric properties of pipe components are usually not allowed to be changed due to the requirements of pipeline design standards [12]. Hence, layout optimization of elastic supports of a pipeline, as a practicable optimization scheme, has received wide attention from scholars [13,14]. Kwong and Edge [15] first employed the layout optimization method to suppress the vibration of a hydraulic pipeline system. They exploited the transfer matrix method (TMM) to establish the numerical model of a fluid-conveying pipeline and employed the genetic algorithm (GA) to optimize the installation locations of elastic supports. Herrmann et al. [16] focused on the effect of support locations on vibration transmission and proposed a novel optimization method for determining the elastic supports based on ANSYS. Tang et al. [17] presented a clamp layout optimization method based on reliability and failure probability to improve the vibration performance of the pipeline system. Gao et al. [18] conducted a global sensitivity analysis of a hydraulic pipeline to determine the effect of support layout on the natural frequencies. Recently, Li et al. [19] tackled the resonance problem of a pipeline-pump system and optimized the locations of its elastic supports by using a chaotic swarm particle optimization algorithm. Moreover, Huang et al. [20], Wang et al. [20], and Zhang et al. [22] also addressed the excessive vibration problem of pipelines and provided different optimization methods for support locations or layouts.

Although well-established and widely used, the layout optimization method for pipeline supports has so far concentrated primarily on introducing a global optimization algorithm into the numerical model of a pipeline system.

This may be thought of as improving the dynamic performance of the pipeline system during the design stage, i.e., pre-manufacture. Little research effort has involved the support layout optimization of pipeline systems during service, i.e., post-manufacture. In fact, there are always noticeable differences between the dynamic behavior of the manufactured and designed pipeline systems [18,23]. Such differences usually arise from manufacturing tolerances and degradation of structural components and may cause the well-designed support layout to perform poorly post-manufacture [12]. Therefore, it is of practical significance to re-optimize the support layout of the post-manufactured pipeline system. This is the objective of the present work.

Generally speaking, it is usually referred to as structural modification technology modifying the physical properties of an existing structure to obtain desirable dynamic performances [24,25]. Among many structural modification techniques, the receptance methodology is powerful and thus frequently used [26]. Such a methodology allows the optimal parameter modifications to be acquired directly from experimental frequency response functions (FRFs) without the need to construct or update a theoretical model of the post-manufactured structure or to perform time-consuming sample calculations [27].

The receptance methodology is first summarized systematically by Ram and Mottershead in a review paper [28], who proposed several modification approaches, including mass modification, grounding spring modification, and connecting spring modification. Subsequently, Caker [29], Ouyang et al. [30,31], Liu et al. [32], Richiedei et al. [33], and Zhang et al. [26] carried out some worthwhile investigations about theoretical research and numerical verifications of the receptance methodology. In recent years, the rapid development of testing techniques has encouraged the practical application of the receptance methodology. Mottershead et al. [34] studied the structural modification problem of a real helicopter tail cone by using the measured receptance. Caracciolo et al. [35] employed the inverse structural modification approach to improving the dynamic performances of a laboratory vibratory linear feeder. Zarraga et al. [36] utilized the receptance method to modify the natural frequency of a brake-clutch system and successfully tackle its friction noise problem. Tsai and Ouyang [37] designed and tested a geared rotor-bearing system to demonstrate the effectiveness of their receptance method and provide experimental insights. Zhang et al. [12] used the receptance-based stiffness modification technique to assign the multiple natural frequencies of a real water-conveying pipeline.

It should be highlighted that the goals of frequency assignment of the aforementioned works are usually achieved by adding or removing mass or stiffness elements at some specific coordinates (named as parameters modification) rather than changing the boundary or support coordinates of the structures (refer to as location optimization in this paper) [38]. However, for an industrial post-manufactured pipeline, the parameter modification technology, even though theoretically effective [12], may not be allowed in practice due to other requirements (such as deflection and stiffness requirements); in contrast, the location or layout optimization of pipeline supports is acceptable and widely used for solving its natural frequency assignment problem [32,37,39].

Notably, previous investigations of location or layout optimization of a post-manufactured pipeline system usually require the construction of its numerical model and updating of the model with the experimental modal or FRF data, for example, in the aforementioned [19]. Such techniques lead to time-consuming calculations, and the obtained results are also constrained to the accuracy of the numerical model. In contrast, this paper employs the receptance methodology and establishes a new layout optimization method that only involves measured modal parameters. In this method, the target of natural frequency assignment is achieved by performing structural modification in two stages. The goal of the first stage of structural modification is to remove the elastic supports of the pipeline (that is, modify the stiffness of pipeline supports to zero) and obtain the FRFs of the pipeline system without elastic supports. This paper achieves such a modification through a virtual parameter modification, which does not require physically removing these elastic supports since the needed FRFs can be estimated by using a typical receptance method. In the second stage of structural modification, the proposed layout optimization method is employed to determine the optimal locations of all elastic supports, and then the desired natural frequency can be obtained by physically realizing these optimal locations. The proposed method is advantageous in more than one way. On the one hand, the proposed method inherits the advantages of measurement-based structural modification techniques, which only require the experimental modal parameters (natural frequencies, damping ratios, and mode shapes) of the post-manufactured pipeline and do not involve the theoretical or numerical model of the pipeline system. Such superiority can help the optimization solution of the pipeline support layout without dependence on the accuracy of a theoretical model. On the other hand, the dynamic behavior of elastic supports can be directly represented by using their measured dynamic stiffness parameters [40], which does not need a pre-determined simplified form.

The remainder of this paper is organized as follows: Section 2 introduces the resonance problem of the pipeline system and the importance of natural frequency assignment and then proposes a new measurement-based layout optimization method. In Section 3, the proposed method is demonstrated numerically on an L-shaped pipeline system with five elastic supports. Next, the experimental validation of this method is provided in Section 4, which highlights its performance and applicability. Finally, conclusions are drawn in Section 5.

2. Structural modification theory in layout optimization of elastic supports

2.1 Problem statement

Generally speaking, a fluid-conveying pipeline system can be viewed as a linear-time-invariant vibrating system and modelled as [12]

$$\mathbf{Z}(\omega)\mathbf{u}(\omega) = (\mathbf{K} + \mathrm{i}\omega\mathbf{C} - (\mathbf{M}_\mathrm{s} + \mathbf{M}_\mathrm{w})\omega^2 + \mathbf{Z}_d(\omega))\mathbf{u}(\omega) = \mathbf{f}(\omega), \tag{1}$$

where $\mathbf{Z}(\omega)\in\Re^{N\times N}$ is usually called the dynamic stiffness matrix of the whole pipeline system; $\mathbf{M}_\mathrm{s}$, $\mathbf{M}_\mathrm{w}\in\Re^{N\times N}$ are the mass matrices of the pipeline structure and the fluid, respectively; $\mathbf{K}$, $\mathbf{C}\in\Re^{N\times N}$ are the stiffness and damping matrices of the pipeline structure, respectively; $\mathbf{Z}_d(\omega)\in\Re^{N\times N}$ is the dynamic stiffness matrix of the attached supports; $\mathbf{u}(\omega)\in\Re^{N}$ represent the displacement response vector of the pipeline system, and $\mathbf{f}(\omega)\in\Re^{N}$ is the excitation force vector acting on the pipeline from the power equipment; i represents the imaginary unit.

It is assumed that the coordinate of the power equipment is q, and its generated external force is denoted as $f_q(\omega)$. Consequently, the vibrating displacement response $u_p(\omega)$ of coordinate p can be written as

$$u_p(\omega) = \mathbf{e}_p^\mathrm{T}\mathbf{H}(\omega)\mathbf{e}_q f_q(\omega) = h_{pq}(\omega) f_q(\omega), \tag{2}$$

where $\mathbf{H}(\omega)=\mathbf{Z}(\omega)^{-1}$ is referred to as the receptance matrix; $\mathbf{e}_q$ represents an N-dimensional unit column vector whose q^{th} element is 1, and the remaining elements are all 0.

It should be highlighted that the power equipment usually consists of a rotor working at a specific operating speed, and the excitation frequencies can be identified from the vibration response spectra (as shown in Fig. 1) [19,23]. Correspondingly, the resonance region of the pipeline system can be estimated in accordance with the technical

standard for avoiding resonance [41]

$$[\omega_{\mathrm{re}}^{L}, \omega_{\mathrm{re}}^{U}] = [(1-\eta)\omega_e, (1+\eta)\omega_e], \tag{3}$$

where ω_e is the excitation frequency of the power equipment; ω_{re}^{L} and ω_{re}^{U} are the lower and upper bounds of the resonance region, respectively; η is the influence coefficient of the excitation frequency. It should be noted that the influence coefficient η for the two excitation frequencies is all set as 10% in this work, which is frequently used in ship industries.

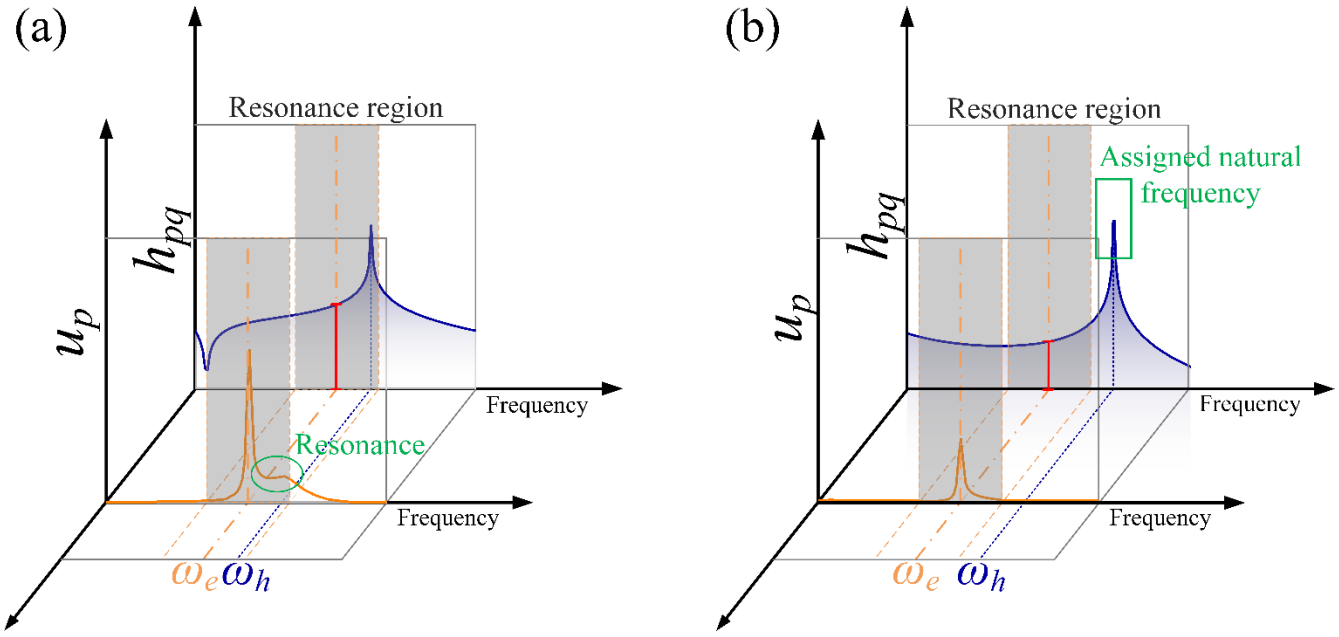

Fig. 1. Schematic diagram of resonance problem of an industrial pipeline system: (a) Reason of resonance phenomena occurring; (b) Resonance avoiding through structural modification technology.

Conventionally, the resonance phenomena occur in the following scenario of Fig. 1a, where a natural frequency ω_h of the pipeline system is within the resonance region of the excitation frequency [42]. Apparently, the vibrating response of the pipeline is amplified in this case. In order to contain the vibration, an effective way is to shift the natural frequency near a frequency of excitation out of the resonance region by performing appropriate structural modifications, reducing the values of the FRFs in the resonance region, as shown in Fig. 1b [12,38]. To do so, two key issues must be addressed:

- Change in the material and geometry of the pipeline structure is not allowed. Only the locations of elastic supports of the pipeline are allowed to be readjusted, especially when this kind of resonance problem occurs in the post-manufacturing stage [18,23].

- The theoretical model may not accurately represent the post-manufactured pipeline system [19,21], especially considering the local deformation and pre-stress effect.

In order to tackle the aforementioned problems, a measurement-based layout optimization method, which does not involve a theoretical (numerical) model of the pipeline system, is proposed, and the optimal locations of its elastic supports are directly found by utilizing the experimental modal parameters. The layout optimization of the pipeline's elastic supports is divided into the following steps shown in Fig. 2.

Since Step 1 can be achieved easily by employing impact hammer tests and a mature modal parameter analysis technology [12,43], Steps 2 and 3 will be elaborated on in the following sections.

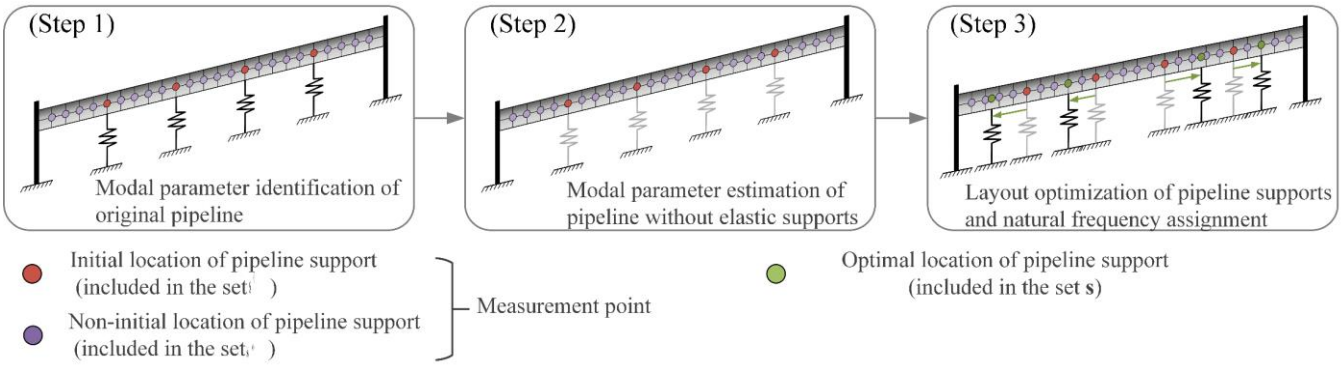

Fig. 2. Executive steps of the layout optimization.

2.2 Modal parameter estimation method of pipeline system without elastic supports

For an existing pipeline system with elastic supports, its FRFs can be measured by employing a modal test, from which the natural frequencies ω_j, damping ratio ξ_j, and mode shapes $\boldsymbol{\varphi}_j$ can be identified by exploiting the modal parameter estimation method [43]. As a result, the receptance matrix can be fitted as

$$\mathbf{H}(\omega)=\mathbf{Z}(\omega)^{-1}\cong\sum_{j=1}^{N_j}\frac{\boldsymbol{\varphi}_j^{\mathrm{T}}\boldsymbol{\varphi}_j}{(\omega^2+2\mathrm{i}\xi_j\omega\omega_j-\omega_j^2)}, \tag{4}$$

where N_j is the number of modes involved in the modal synthesis.

Now, it is assumed that the elastic supports attached to the pipeline are removed, and then the receptance matrix of the pipeline system without elastic supports can be expressed as

$$\bar{\mathbf{H}}(\omega) = \bar{\mathbf{Z}}(\omega)^{-1} = (\mathbf{K} + \mathrm{i}\omega\mathbf{C} - (\mathbf{M}_s + \mathbf{M}_w)\omega^2)^{-1}, \tag{5}$$

where $\bar{\mathbf{Z}}(\omega)$ is the dynamic stiffness matrix of the pipeline system without elastic supports.

Obviously, Eq. (5) can be written as

$$\bar{\mathbf{H}}(\omega) = \bar{\mathbf{Z}}(\omega)^{-1} = (\mathbf{Z}(\omega) - \mathbf{Z}_d(\omega))^{-1}, \tag{6}$$

Substituting Eq. (4) into Eq. (6) leads to

$$\bar{\mathbf{H}}(\omega) = (\mathbf{I} - \mathbf{H}(\omega)\mathbf{Z}_d(\omega))^{-1}\mathbf{H}(\omega). \tag{7}$$

It should be highlighted that the initial location coordinates of all elastic supports are known, and their dynamic stiffness parameters also can be obtained directly via a vibration test before installation [40]. Theoretically, the FRFs of pipeline systems without elastic supports can be calculated using Eq. (7). However, some numerical errors are inevitably accumulated when employing the MATLAB program to solve Eq. (7) since Eq. (7) contains the inverse operation of super-large matrices [32]. In order to reduce their numerical errors, this paper considers solving $\bar{\mathbf{H}}(\omega)$ in blocks.

It is assumed that a total of r elastic supports are attached to the pipeline. For arbitrary elastic support, its initial attachment location and dynamic stiffness are denoted as s^0 and $z(\omega)$, respectively. Then, the initial support layout of the pipeline system is conveniently denoted as $\mathbf{s}^0 = [s_1^0, s_2^0, \cdots, s_r^0]^{\mathrm{T}} \in \Re^r$; in contrast, the remaining locations other than the elastic supports can be collected in $\check{\mathbf{s}}^0 \in \Re^{N-r}$, as shown in Fig. 2. After the elementary transformation of matrices [26], the receptance matrix of the initial layout can be expressed as

$$\mathbf{H}(\omega) = \begin{bmatrix} \mathbf{H}_{\check{\mathbf{s}}^0\check{\mathbf{s}}^0}(\omega) & \mathbf{H}_{\mathbf{s}^0\check{\mathbf{s}}^0}(\omega) \\ \mathbf{H}_{\check{\mathbf{s}}^0\mathbf{s}^0}(\omega) & \mathbf{H}_{\mathbf{s}^0\mathbf{s}^0}(\omega) \end{bmatrix}. \tag{8}$$

Additionally, the dynamic stiffness matrix of these elastic supports can be denoted as

$$\mathbf{Z}_d(\omega)=\begin{bmatrix}\mathbf{0} & \mathbf{0}\\ \mathbf{0} & \mathbf{Z}_{rr}(\omega)\end{bmatrix}, \tag{9}$$

where $\mathbf{Z}_{rr}(\omega)$ is the non-singular submatrix of $\mathbf{Z}_d(\omega)$, denoted as $\text{diag}([z_1(\omega), z_2(\omega),\cdots,z_r(\omega)])\in\Re^{r\times r}$.

Substituting Eq. (8) and (9) into Eq. (7) yields

$$\bar{\mathbf{H}}(\omega)=\begin{bmatrix}\bar{\mathbf{H}}_{\check{\mathbf{s}}^0\check{\mathbf{s}}^0}(\omega) & \bar{\mathbf{H}}_{\check{\mathbf{s}}^0\mathbf{s}^0}(\omega)\\ \bar{\mathbf{H}}_{\mathbf{s}^0\check{\mathbf{s}}^0}(\omega) & \bar{\mathbf{H}}_{\mathbf{s}^0\mathbf{s}^0}(\omega)\end{bmatrix}=\begin{bmatrix}\mathbf{H}_{\check{\mathbf{s}}^0\check{\mathbf{s}}^0}+\mathbf{H}_{\check{\mathbf{s}}^0\mathbf{s}^0}\mathbf{Z}_{rr}(\mathbf{I}_{rr}-\mathbf{H}_{\mathbf{s}^0\mathbf{s}^0}\mathbf{Z}_{rr})^{-1}\mathbf{H}_{\mathbf{s}^0\check{\mathbf{s}}^0} & \mathbf{H}_{\check{\mathbf{s}}^0\mathbf{s}^0}(\mathbf{I}_{rr}-\mathbf{H}_{\mathbf{s}^0\mathbf{s}^0}\mathbf{Z}_{rr})^{-1}\\ (\mathbf{I}_{rr}-\mathbf{H}_{\mathbf{s}^0\mathbf{s}^0}\mathbf{Z}_{rr})^{-1}\mathbf{H}_{\mathbf{s}^0\check{\mathbf{s}}^0} & (\mathbf{I}_{rr}-\mathbf{H}_{\mathbf{s}^0\mathbf{s}^0}\mathbf{Z}_{rr})^{-1}\mathbf{H}_{\mathbf{s}^0\mathbf{s}^0}\end{bmatrix}. \tag{10}$$

Correspondingly, the FRF $\bar{h}_{pq}(\omega)$ of the pipeline system without elastic supports can be predicted by exploiting the following Eq. (11).

$$\bar{h}_{pq}(\omega)=\mathbf{e}_p^{\mathrm{T}}\bar{\mathbf{H}}(\omega)\mathbf{e}_q=\mathbf{e}_p^{\mathrm{T}}\begin{bmatrix}\bar{\mathbf{H}}_{\check{\mathbf{s}}^0\check{\mathbf{s}}^0}(\omega) & \bar{\mathbf{H}}_{\check{\mathbf{s}}^0\mathbf{s}^0}(\omega)\\ \bar{\mathbf{H}}_{\mathbf{s}^0\check{\mathbf{s}}^0}(\omega) & \bar{\mathbf{H}}_{\mathbf{s}^0\mathbf{s}^0}(\omega)\end{bmatrix}\mathbf{e}_q. \tag{11}$$

Finally, the modal parameters of the pipeline system without elastic supports are obtained by using the estimation method, denoting as $(\bar{\omega}_j, \bar{\xi}_j, \bar{\boldsymbol{\varphi}}_j)$ [44]. It should be stressed that the aforementioned structural modification is a kind of virtual modification where there is no need to remove these elastic supports physically. In this way, the workload involved in Step 2 is reduced, and simultaneously, the risk of excessive stresses appearing on the pipeline due to the removal of pipeline supports can be avoided.

Notably, the estimated mode shape vector $\bar{\boldsymbol{\varphi}}_j\in\Re^N$ only contains the mode shape values at those measurement points and does not involve those at other non-observed points [12]. Hence, a widely-used polynomial fitting method is exploited to evaluate the mode shape components at other non-observed points [45]. As a consequence, the j^{th} mode shape component of an arbitrary location s on the pipeline without elastic supports can be expressed as

$$\bar{\varphi}_j(s)=\sum_{b=1}^{m}a_{j,b}s^{(b-1)}, \tag{12}$$

where $a_{j,b}$ is the b^{th} polynomial fitting coefficients. It should be noted that the number of measurement points related to the mode function fitting (N) should be greater than the mode number (j) in order to ensure the accuracy of the fitted mode shape function.

2.3 Calculation method for the optimal layout of pipeline supports

After obtaining the modal parameters of the pipeline without elastic supports, this work aims to realize the natural frequency assignment by relocating appropriate elastic supports. Now, it is assumed to impose a new support layout $\mathbf{s}=[s_1,s_2,\cdots,s_r]$ to the pipeline system, and then the receptance matrix of the pipeline system at the new layout can be expressed as

$$\widetilde{\mathbf{H}}(\omega,\mathbf{s}) =(\mathbf{I}+\overline{\mathbf{H}}(\omega)\mathbf{Z}_d^{\mathbf{s}}(\omega))^{-1}\overline{\mathbf{H}}(\omega). \tag{13}$$

where $\mathbf{Z}_d^{\mathbf{s}}(\omega)$ is the dynamic stiffness matrix of the attached supports at the new support layout $\mathbf{s}$.

Re-arranging Eq. (13) leads to

$$\begin{aligned}\widetilde{\mathbf{H}}(\omega,\mathbf{s}) &= \begin{bmatrix}\widetilde{\mathbf{H}}_{\check{\mathbf{s}}\check{\mathbf{s}}}(\omega) & \widetilde{\mathbf{H}}_{\check{\mathbf{s}}\mathbf{s}}(\omega)\\ \widetilde{\mathbf{H}}_{\mathbf{s}\check{\mathbf{s}}}(\omega) & \widetilde{\mathbf{H}}_{\mathbf{ss}}(\omega)\end{bmatrix}\\ &= \left[\begin{bmatrix}\mathbf{I}_{(N-r)(N-r)} & \mathbf{0}\\ \mathbf{0} & \mathbf{I}_{rr}\end{bmatrix}+\begin{bmatrix}\overline{\mathbf{H}}_{\check{\mathbf{s}}\check{\mathbf{s}}}(\omega) & \overline{\mathbf{H}}_{\check{\mathbf{s}}\mathbf{s}}(\omega)\\ \overline{\mathbf{H}}_{\mathbf{s}\check{\mathbf{s}}}(\omega) & \overline{\mathbf{H}}_{\mathbf{ss}}(\omega)\end{bmatrix}\begin{bmatrix}\mathbf{0} & \mathbf{0}\\ \mathbf{0} & \mathbf{Z}_{rr}(\omega)\end{bmatrix}\right]^{-1}\begin{bmatrix}\overline{\mathbf{H}}_{\check{\mathbf{s}}\check{\mathbf{s}}}(\omega) & \overline{\mathbf{H}}_{\check{\mathbf{s}}\mathbf{s}}(\omega)\\ \overline{\mathbf{H}}_{\mathbf{s}\check{\mathbf{s}}}(\omega) & \overline{\mathbf{H}}_{\mathbf{ss}}(\omega)\end{bmatrix}.\end{aligned} \tag{14}$$

After simplification, Eq. (14) can be written as

$$\widetilde{\mathbf{H}}(\omega,\mathbf{s}) = \begin{bmatrix}\widetilde{\mathbf{H}}_{\check{\mathbf{s}}\check{\mathbf{s}}}(\omega) & \widetilde{\mathbf{H}}_{\check{\mathbf{s}}\mathbf{s}}(\omega)\\ \widetilde{\mathbf{H}}_{\mathbf{s}\check{\mathbf{s}}}(\omega) & \widetilde{\mathbf{H}}_{\mathbf{ss}}(\omega)\end{bmatrix} = \begin{bmatrix}\mathbf{I}_{(N-r)(N-r)} & \overline{\mathbf{H}}_{\check{\mathbf{s}}\mathbf{s}}(\omega)\mathbf{Z}_{rr}(\omega)\\ \mathbf{0} & \mathbf{I}_{rr}+\overline{\mathbf{H}}_{\mathbf{ss}}(\omega)\mathbf{Z}_{rr}(\omega)\end{bmatrix}^{-1}\begin{bmatrix}\overline{\mathbf{H}}_{\check{\mathbf{s}}\check{\mathbf{s}}}(\omega) & \overline{\mathbf{H}}_{\check{\mathbf{s}}\mathbf{s}}(\omega)\\ \overline{\mathbf{H}}_{\mathbf{s}\check{\mathbf{s}}}(\omega) & \overline{\mathbf{H}}_{\mathbf{ss}}(\omega)\end{bmatrix}. \tag{15}$$

Suppose that $\widetilde{\omega}_t$ is the target natural frequency, known from the requirement of resonance avoidance. The goal of the natural frequency assignment is to find the optimal support layout $\mathbf{s}=[s_1,s_2,\cdots,s_r]$ to realize the target natural frequency. Such a problem is an inverse problem of solving the required support locations $\mathbf{s}$.

Considering $\widetilde{\omega}_t$ is a natural frequency of the pipeline system with the optimal support layout $\mathbf{s}$, it theoretically satisfies the following Eq. (16) [26,28,32].

$$\det\left(\begin{bmatrix}\mathbf{I}_{(N-r)(N-r)} & \overline{\mathbf{H}}_{\check{\mathbf{s}}\mathbf{s}}(\widetilde{\omega}_t)\mathbf{Z}_{rr}(\widetilde{\omega}_t)\\ \mathbf{0} & \mathbf{I}_{rr}+\overline{\mathbf{H}}_{\mathbf{ss}}(\widetilde{\omega}_t)\mathbf{Z}_{rr}(\widetilde{\omega}_t)\end{bmatrix}\right)=0. \tag{16}$$

In order to save the computational cost of equation solving, the dimensions of matrices involved in Eq. (16) are reduced, and the simplified equation can be expressed as

$$\det(\mathbf{I}_{rr}+\bar{\mathbf{H}}_{\mathbf{ss}}(\tilde{\omega}_t)\mathbf{Z}_{rr}(\tilde{\omega}_t))=0, \tag{17}$$

where $\mathbf{Z}_{rr}(\tilde{\omega}_t)=\mathrm{diag}([z_1(\tilde{\omega}_t), z_2(\tilde{\omega}_t),\cdots,z_r(\tilde{\omega}_t)])\in\Re^{r\times r}$ is the dynamic stiffness matrix of these elastic supports at the frequency $\tilde{\omega}_t$, which is a non-singular matrix; $\bar{\mathbf{H}}_{\mathbf{ss}}(\tilde{\omega}_t)\in\Re^{r\times r}$ is the partial receptance matrix composing these cross and point FRFs at the support locations **s**, which can be approximated as

$$\bar{\mathbf{H}}_{\mathbf{ss}}(\tilde{\omega}_t)=\sum_{j=1}^{N_j}\frac{\bar{\boldsymbol{\varphi}}_{j,r}^{\mathrm{T}}(\mathbf{s})\bar{\boldsymbol{\varphi}}_{j,r}(\mathbf{s})}{(\tilde{\omega}_t^2+2\mathrm{i}\bar{\xi}_j\tilde{\omega}_t\bar{\omega}_j-\bar{\omega}_j^2)}, \tag{18}$$

where $\bar{\boldsymbol{\varphi}}_{j,r}(\mathbf{s})$ is the mode shape components of support locations **s** [12] and can be described by employing Eq. (12) as

$$\begin{aligned}\bar{\boldsymbol{\varphi}}_{j,r}(\mathbf{s})&=[\bar{\varphi}_j(s_1),\bar{\varphi}_j(s_2),\cdots,\bar{\varphi}_j(s_r)]^{\mathrm{T}}\\&=\left[\sum_{b=1}^{m}a_{j,t}(s_1)^{(b-1)},\sum_{b=1}^{m}a_{j,t}(s_2)^{(b-1)},\cdots,\sum_{b=1}^{m}a_{j,t}(s_r)^{(b-1)}\right]^{\mathrm{T}}.\end{aligned} \tag{19}$$

By substituting Eq. (18) and (19) into Eq. (17), it is clear that Eq. (17) is a multivariate nonlinear equation only related to optimal support location **s**, and its solvability is not ensured since the potential rank-mismatching problem [30,46]. Hence, in order to find the optimal locations conveniently, the equation-solving problem is cast as a multiobjective optimization (MOP) problem [12,26]

$$\begin{aligned}&\text{minimize } \boldsymbol{\Psi}(\mathbf{s})=\left[\Psi_1(\mathbf{s}),\Psi_2(\mathbf{s}),\cdots,\Psi_{N_s}(\mathbf{s})\right]^{\mathrm{T}},\\&\text{subject to } \mathbf{s}\in\boldsymbol{\Gamma},\end{aligned} \tag{20}$$

where $\boldsymbol{\Gamma}$: $\mathbf{s}^L\le\mathbf{s}\le\mathbf{s}^U$ is the feasible domain of the support locations, which can be determined in accordance with the initial location of the elastic support and actual engineering requirements ; N_s is the number of target natural frequencies (sub-objective), and the t^{th} sub-objective function is defined as

$$\Psi_t(\mathbf{s})=\|\mathbf{I}_{rr}+\bar{\mathbf{H}}_{\mathbf{ss}}(\tilde{\omega}_t)\mathbf{Z}_{rr}(\tilde{\omega}_t)\|_2. \tag{21}$$

The optimal locations **s** can be solved by exploiting a multiobjective optimization algorithm to minimize the objective-function vector $\boldsymbol{\Psi}(\mathbf{s})$. As far as this work is concerned, a widely-used global optimization algorithm, the NSGA-II algorithm, is employed to solve this MOP problem. The developments and important features of the

NSGA-II algorithm can be found in Refs. [26,47] and are not presented here.

An overview of the layout optimization method is illustrated in Fig. 3.

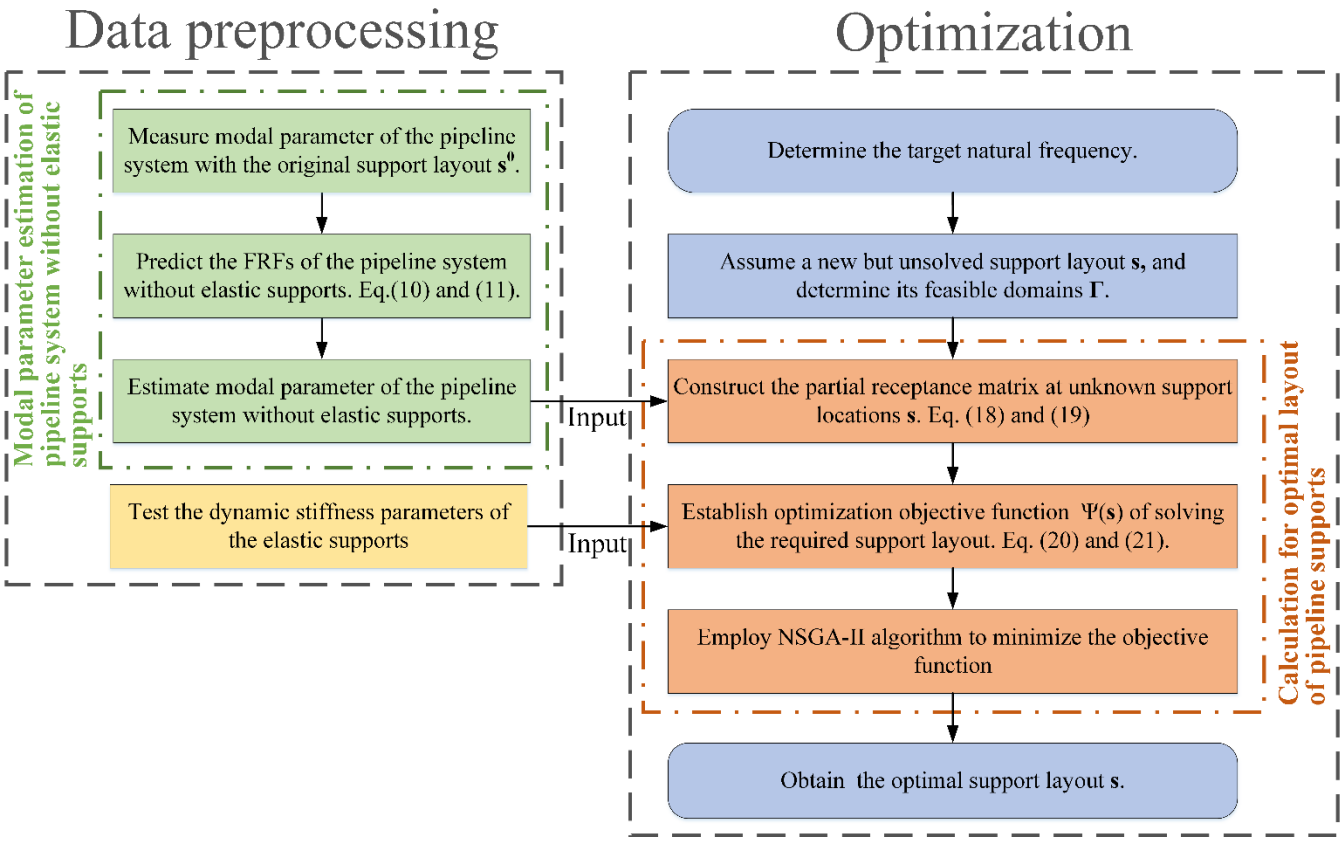

Fig. 3. Method overview.

3 Numerical analysis

In this section, a numerical pipeline system is employed to prove the effectiveness of the proposed method. It should be noted that the required FRFs in this section are obtained from theoretical models, but in practice, they can be directly measured quite easily.

3.1 Numerical model

Consider an L-shaped pipeline system frequently used in modern industry, as shown in Fig. 4a. This pipeline system,

whose two ends are clamped rigidly, is connected to the ground through five elastic supports of the same type. These five elastic supports are named z_1–z_5, and their initial attachment locations on the pipeline are denoted correspondingly as s_1^0–s_5^0.

The pipeline material is 304L stainless steel, and the filled liquid inside is water. The system parameters of the two materials are collected in Table 1. It should be noted that the effect of the low flow speed, common in the industry, on the dynamics of the pipeline is marginal and is ignored in this paper [12,45].

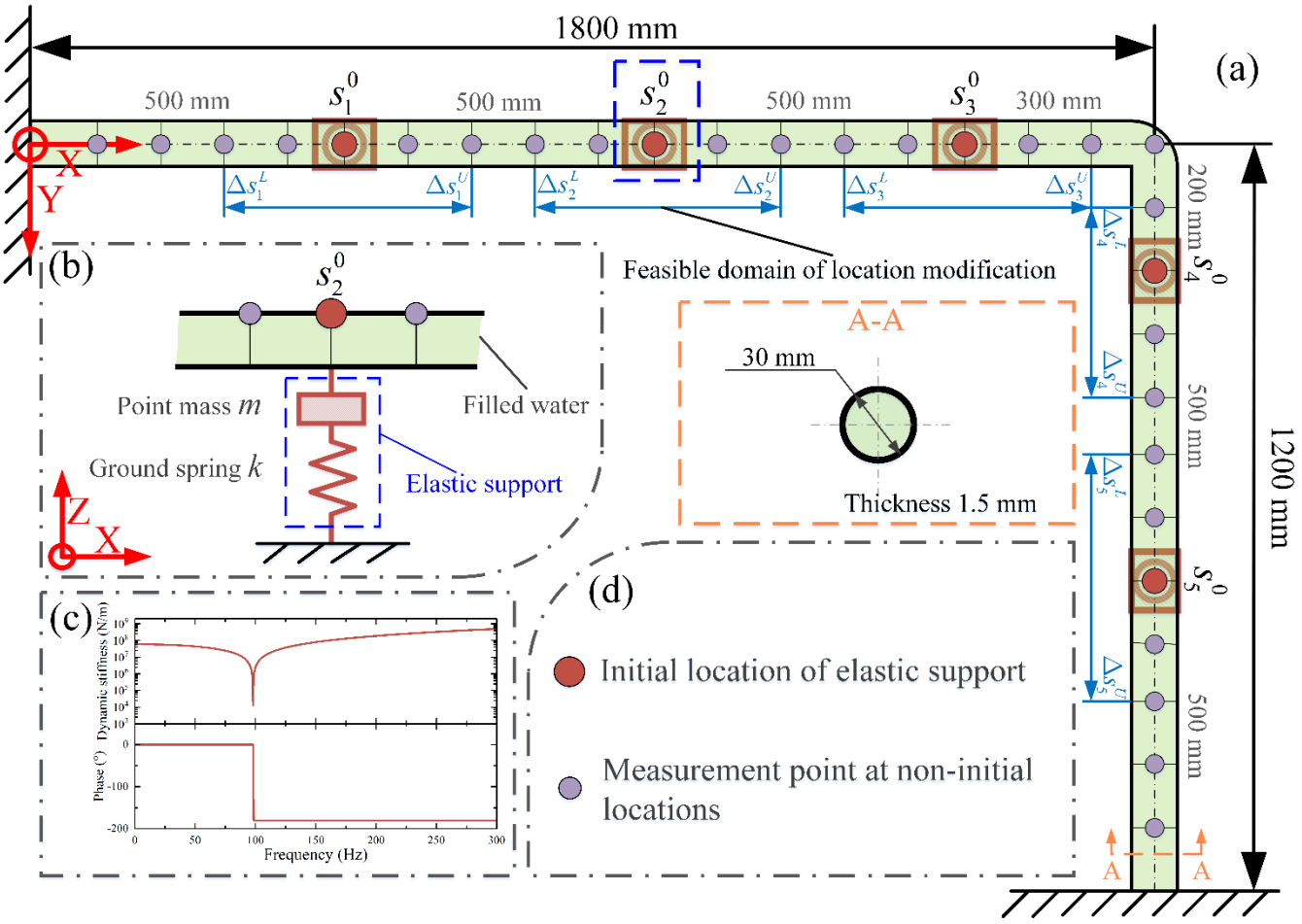

Fig. 4. L-shaped pipeline system with elastic supports: (a) geometry of pipeline system; (b) components of elastic support; (c) dynamic stiffness of elastic support; (d) indicator of measurement points.

For parameterization purposes, the elastic support is modelled as an assembly of a point mass m weighing 0.22 kg and a ground spring k with a stiffness of 59.16 kN/m, as shown in Fig. 4b. Its dynamic stiffness parameter curve is

displayed in Fig. 4c.

Table 1. System parameters of the pipeline and filled water.

	Density	Young's modulus	Poisson's ratio	Flow speed
Pipeline	7850 kg/m^3	187 GPa	0.33	-
Filled water	1000 kg/m^3	-	-	0.0 m/s

Generally speaking, the excitation direction of the power equipment is parallel to the support installation direction (Z-direction in this paper), and the vibration of the pipeline in this direction is of industrial concern [12,23]. Hence, this paper aims to modify the dynamic behaviour of the Z-direction to solve the pipeline's resonance problem in this direction.

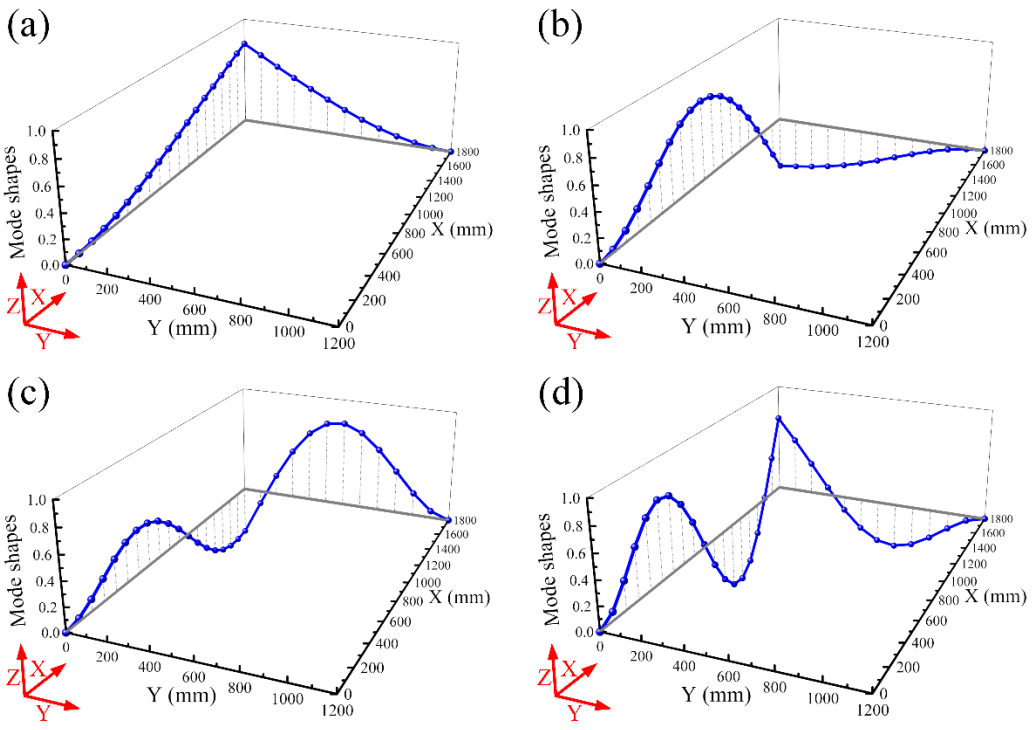

Fig. 5. First four mode shapes of the original pipeline system: (a) Mode 1; (b) Mode 2; (c) Mode 3; (d) Mode 4.

A total of 29 observation points, including measurement points and initial locations of the elastic supports, are distributed along the pipeline, as shown in Fig. 4a and d. Subsequently, the transfer matrix method (TMM) [12] is employed to determine the FRFs of those observation points. By using the modal parameter identification method

described in [43,44], the first four natural frequencies and corresponding mode shapes are obtained and shown in Table 2 and Fig. 5, respectively.

Table 2. First four natural frequencies and the target frequencies.

	Natural frequency	Whether in resonance	Target frequency
Mode 1	37.83 Hz	Yes	34 Hz
Mode 2	49.47 Hz	Yes	52 Hz
Mode 3	78.11 Hz	No	-
Mode 4	106.77 Hz	No	-

Fig. 6 displays the FRFs of the original pipeline system ($h_{s_1^0 s_1^0}$ and $h_{s_1^0 s_5^0}$) as well as the fitted ones from the estimated modal parameters. The fitted FRFs are in good agreement with the calculated ones, proving the accuracy of the identified modal parameters.

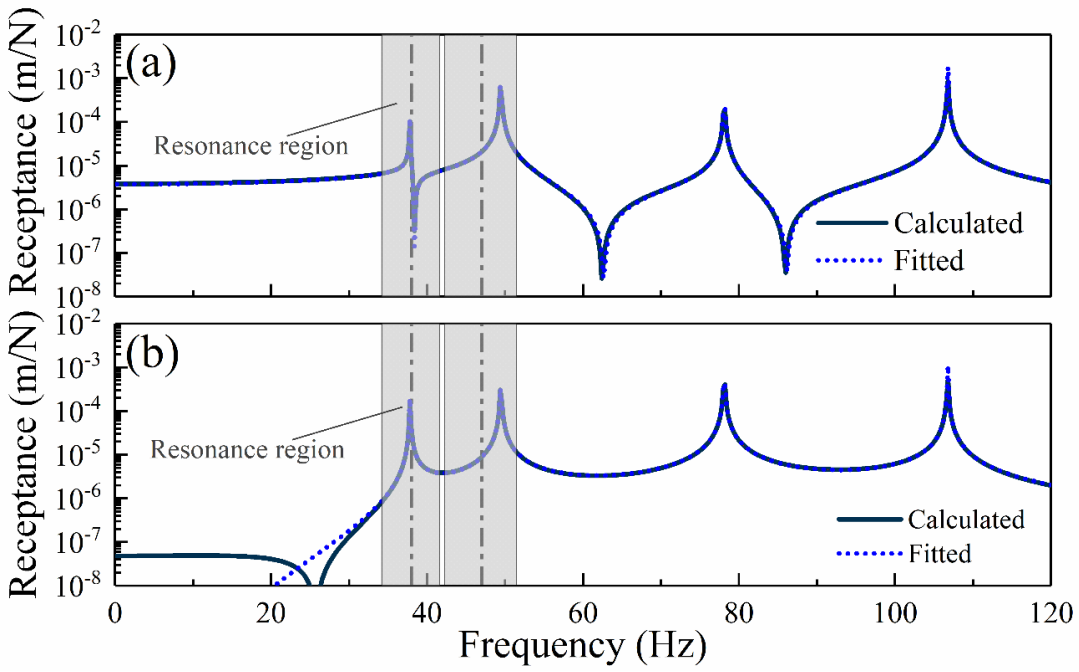

Fig. 6. Comparison between the calculated and fitted FRF: (a) $h_{s_1^0 s_1^0}$; (b) $h_{s_1^0 s_5^0}$.

The pipeline is assumed to be subjected to two different excitations, whose corresponding frequencies are 38 Hz and 47 Hz. By using Eq. (3), the resonance regions of these two excitation frequencies are [34.2, 41.8] Hz and [42.3,

51.7] Hz, respectively, as shown in the shaded area of Fig. 6. Clearly, the pipeline's first and second natural frequencies fall into these resonance regions. Therefore, the goal of this work is to shift the first natural frequency to 34 Hz and the second one to 52 Hz to solve such a resonance problem.

As far as this work is concerned, such a target of natural frequency assignment is expected to be realized by employing the layout optimization of these elastic supports. The initial location coordinates of all elastic supports and the corresponding feasible regions of modifications are listed in Table 3.

Table 3. Initial location coordinates of elastic supports and the corresponding feasible domains of modifications.

	s_1 (mm)	s_2 (mm)	s_3 (mm)	s_4 (mm)	s_5 (mm)
Initial coordinate $(x_{s_i^0},\ y_{s_i^0})$	(500, 0)	(1000, 0)	(1500, 0)	(1800, 200)	(1800, 700)
Feasible domain in X direction	[400, 700]	[800, 1200]	[1300, 1700]	[1800, 1800]	[1800, 1800]
Feasible domain in Y direction	[0, 0]	[0, 0]	[0, 0]	[100, 400]	[500, 900]

3.2 Layout optimization of the elastic supports of the simulated pipeline

By substituting the dynamic stiffness parameters in Fig. 4c into Eq. (10), the receptance matrix of the L-shaped pipeline system without elastic supports is obtained. In order to demonstrate the accuracy of these predicted FRFs, the real FRFs of this pipeline system without elastic supports are calculated, and the obtained results are compared with these predicted ones and shown in Fig. 7. It is found that there is very good agreement between the real and predicted FRFs, both in terms of magnitude and phase.

The modal parameter estimation technique recently proposed in [44] is adopted to identify the eigenstructure of the pipeline system without elastic supports from the predicted FRFs. For benchmark purposes, the real eigenstructure of this pipeline system is also obtained by performing the modal analysis directly for the pipeline without elastic supports. The natural frequencies and mode shapes obtained by the two techniques are shown in Table 4 and Fig. 8, respectively. Clearly, the estimated first and fourth natural frequencies are slightly different from the real ones. It is hypothesized that these differences are caused by round-off errors in the inverse calculation in Eq. (10). Since these errors are marginal (no more than 1%), the proposed modal parameter estimation method (Eqs. (10) and (11)) is trustworthy.

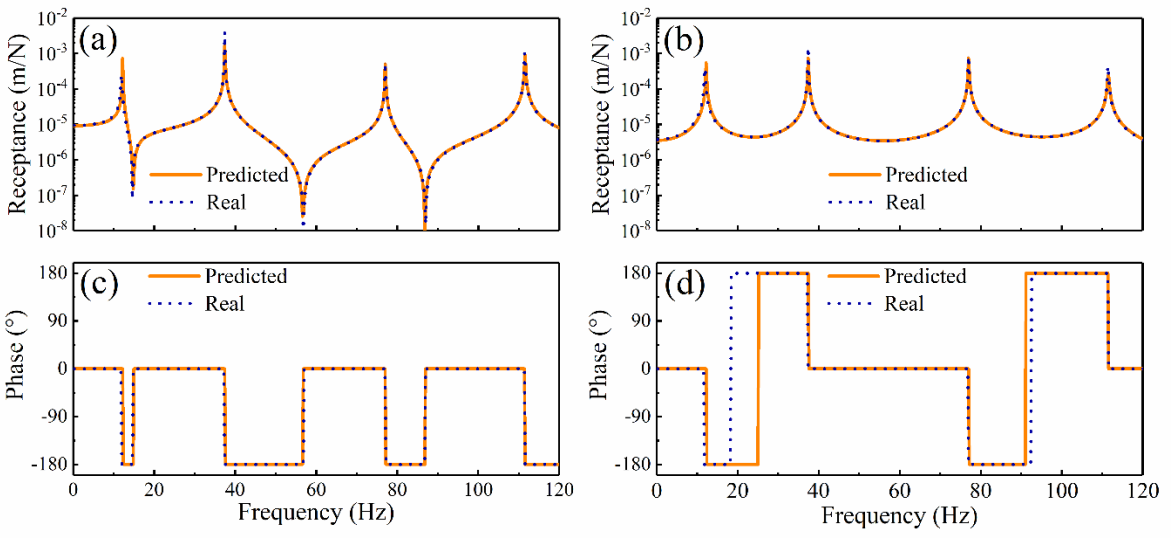

Fig. 7. Predicted and real FRFs of the pipeline system without elastic supports: (a) amplitude of $h_{s_1^0 s_1^0}$; (b) amplitude of $h_{s_1^0 s_5^0}$; (c) phase of $h_{s_1^0 s_1^0}$; (d) phase of $h_{s_1^0 s_5^0}$.

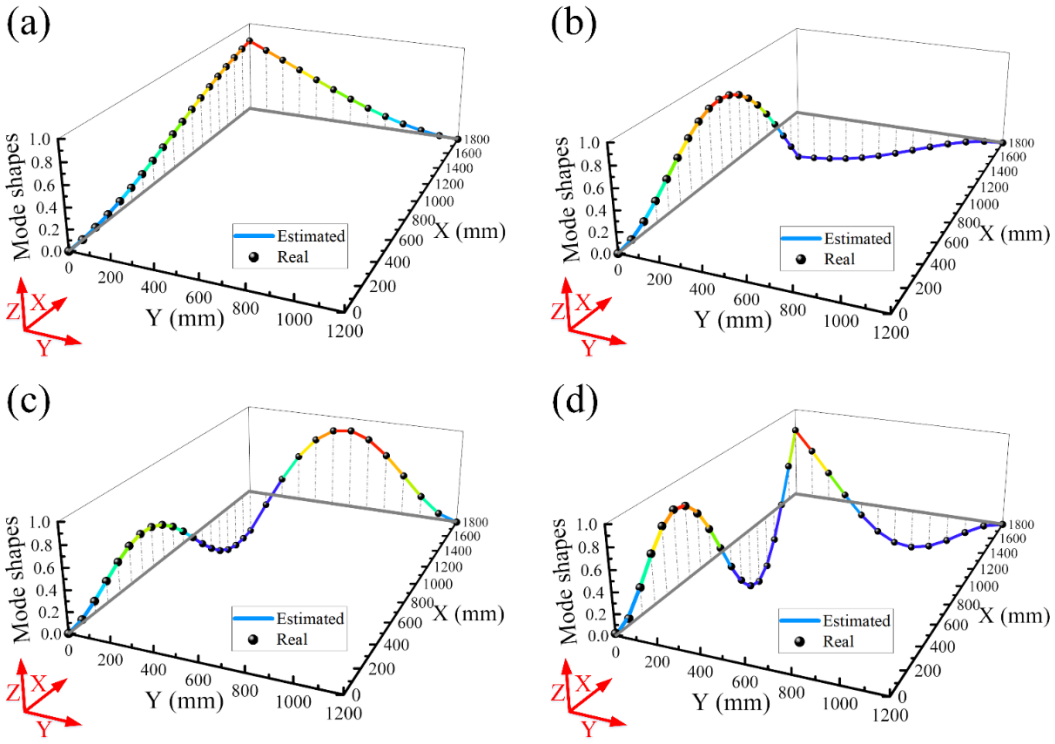

Fig. 8. First four mode shapes of the L-shaped pipeline system without elastic supports: (a) Mode 1; (b) Mode 2; (c) Mode 3; (d) Mode 4.

Table 4. First four natural frequencies of the L-shaped pipeline system without elastic supports.

	Mode 1	Mode 2	Mode 3	Mode 4
Real	11.92 Hz	37.38 Hz	77.05 Hz	111.63 Hz
Estimated	12.03 Hz	37.38 Hz	77.05 Hz	111.57 Hz
Error	0.92%	0.00%	0.00%	0.05%

With the estimated eigenstructure, the mode shape components at arbitrary location s (x, y) are fitted through Eq. (12) and listed in Table 5.

Table 5. Mode shape function of the pipeline system without elastic supports[a].

	Mode shape function
Mode 1	$\begin{cases} -1.91e^{-14}x^4 - 2.63e^{-10}x^3 + 6.84e^{-7}x^2 + 1.05e^{-6}x, & 0 \le x \le 1800,\ y = 0 \\ 1.42e^{-13}y^4 - 1.47e^{-10}y^3 - 1.78e^{-7}y^2 - 8.40e^{-4}y + 0.80, & x = 0,\ 0 \le y \le 1200 \end{cases}$
Mode 2	$\begin{cases} -9.81e^{-13}x^4 - 2.11e^{-9}x^3 + 3.02e^{-6}x^2 + 2.10e^{-5}x, & 0 \le x \le 1800,\ y = 0 \\ -9.78e^{-13}y^4 + 1.15e^{-9}y^3 - 2.51e^{-8}y^2 - 1.64e^{-4}y - 0.56, & x = 0,\ 0 \le y \le 1200 \end{cases}$
Mode 3	$\begin{cases} 4.19e^{-13}x^4 - 5.51e^{-9}x^3 + 4.15e^{-6}x^2 - 7.68e^{-5}x, & 0 \le x \le 1800,\ y = 0 \\ -3.75e^{-12}y^4 - 4.46e^{-9}y^3 + 7.75e^{-7}y^2 - 3.50e^{-3}y - 0.49, & x = 0,\ 0 \le y \le 1200 \end{cases}$
Mode 4	$\begin{cases} -2.23e^{-11}x^4 - 3.32e^{-8}x^3 + 1.64e^{-5}x^2 - 9.18e^{-4}x, & 0 \le x \le 1800,\ y = 0 \\ 1.51e^{-11}y^4 - 4.49e^{-9}y^3 - 1.66e^{-7}y^2 - 2.10e^{-3}y + 0.76, & x = 0,\ 0 \le y \le 1200 \end{cases}$

[a]. the superscript represents power.

Eq. (18) is employed to describe the partial receptance matrices $\bar{\mathbf{H}}_{ss}(2\pi\times34)$ and $\bar{\mathbf{H}}_{ss}(2\pi\times52)$ of these unsolved support locations. Consequently, the objective functions of natural frequency assignment are established through Eq. (20), and the NSGA-II algorithm is used to search for the optimal solutions to such a constrained minimization problem. The population number of the algorithm is set to 50, and the number of running generations to 200. All related calculations, including data preprocessing and optimization calculation, are completed on a personal computer with a 2.30 GHz CPU and 8.0 GB physical memory. The calculation time of the whole optimization is 8.47 s, and the obtained Pareto-optimal front [47] is shown in Fig. 9. It is clear from Fig. 9 that the proposed layout optimization algorithm has the advantage of a fast convergence speed and high accuracy.

The solution with the lowest objective function values (as marked in Fig. 9) is selected as the final layout scheme of elastic supports, and the corresponding optimal locations of elastic supports are listed in Table 6.

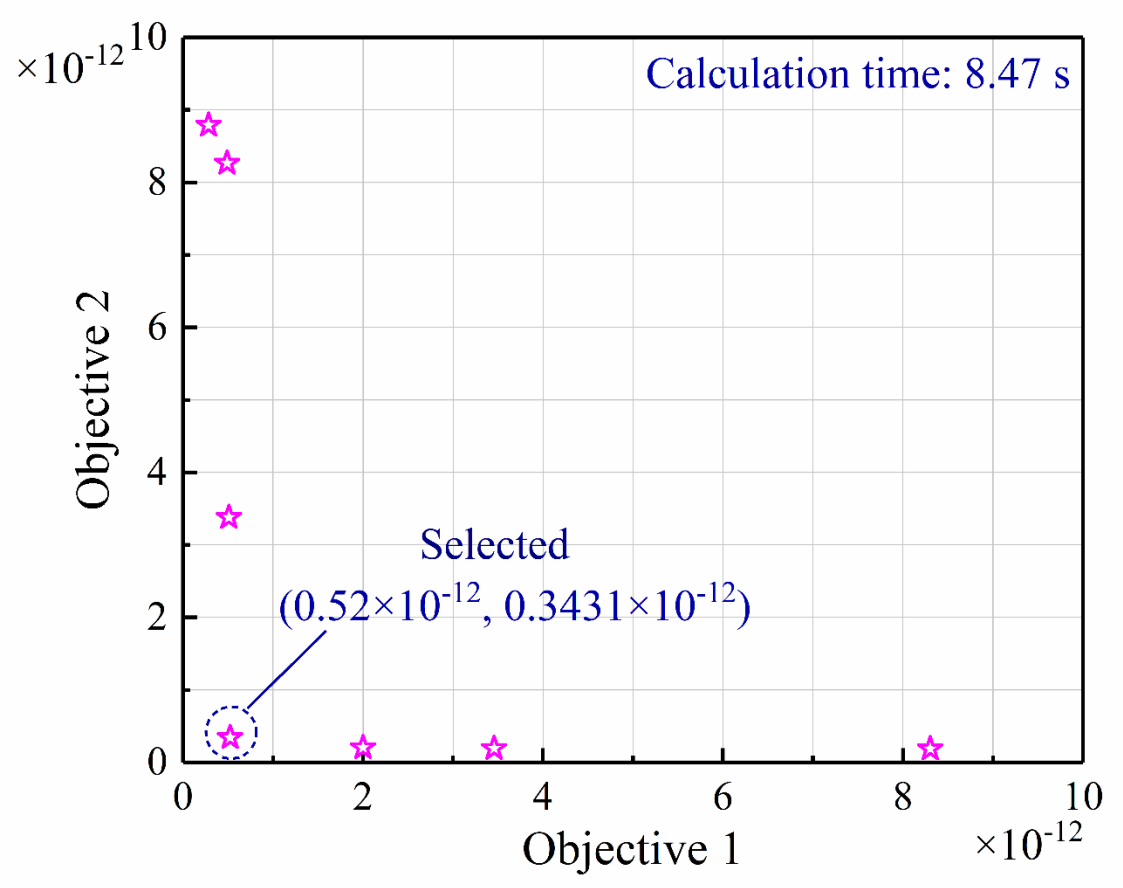

Fig. 9. Pareto optimal front of the layout optimization.

Table 6. Nominal values of the optimal locations of these elastic supports.

Optimal location	s_1	s_2	s_3	s_4	s_5
Nominal value of x (mm)	500 + 121.3	1000 - 76.5	1500 - 160.3	1800.0	1800.0
Nominal value of y (mm)	0.0	0.0	0.0	200 + 95.0	700 - 106.3

After performing these optimal locations numerically, the layout optimization of the pipeline supports is achieved, as shown in Fig. 10.

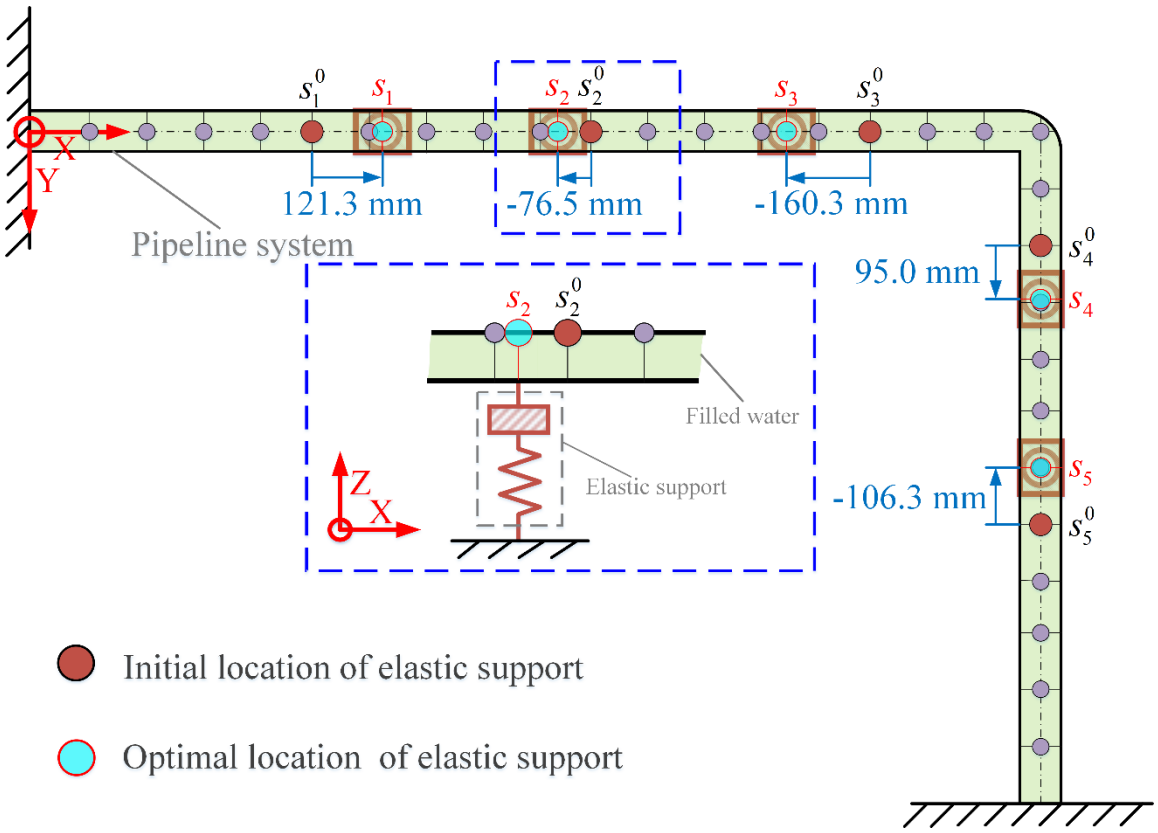

Fig. 10. Locations of these elastic supports before and after layout optimization.

Fig. 11 displays the FRFs $h_{s_1s_1}$ and $h_{s_1s_5}$ of the pipeline system with the optimal layout of elastic supports, from which the natural frequencies of the modified pipeline system are estimated by the peak picking method [37] and collected in Table 7. Notably, the first two natural frequencies of the modified pipeline system have been shifted exactly to the desired frequencies. Such a result demonstrates the effectiveness of the proposed layout optimization method in natural frequency assignment and resonance avoidance of pipelines.

Table 7. First four natural frequencies of the modified pipeline system.

	Natural frequency	Whether in resonance	Target frequency
Mode 1	34.00 Hz	No	34.00 Hz
Mode 2	52.00 Hz	No	52.00 Hz
Mode 3	78.41 Hz	No	-
Mode 4	106.67 Hz	No	-

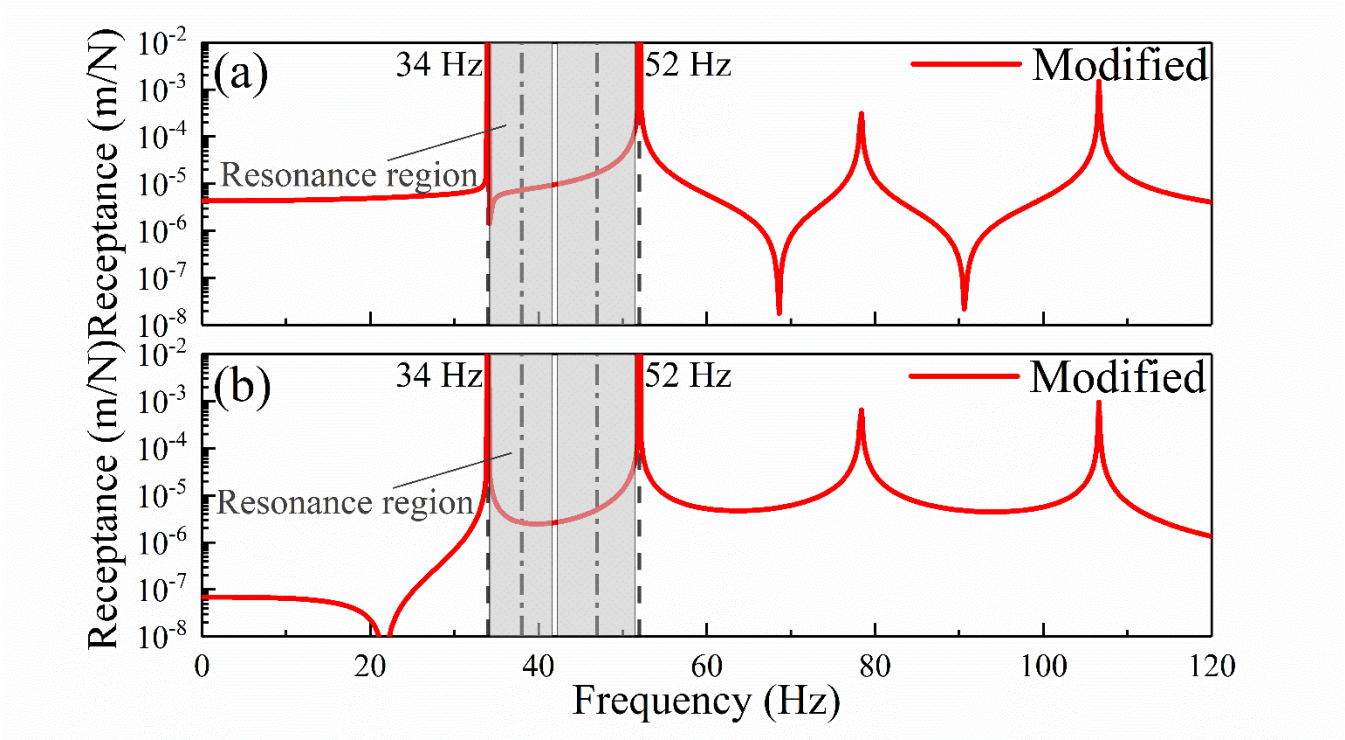

Fig. 11. FRFs of the modified pipeline system: (a) $h_{s_1 s_1}$; (b) $h_{s_1 s_5}$.

4. Experimental validation

4.1 Experimental setup

The proposed method is implemented and validated on an experimental pipeline system, which is displayed in Fig. 12a. This setup consists of two main components:

- The fixed-ends pipeline structure, whose geometry is the same as that of the numerical model in Section 3.1;
- Five spring-damper shock absorbers of the same type, which is a kind of common elastic support in engineering [12,22]. Used elastic support is shown in Fig. 12b.

The system parameters of the experimental pipeline are equivalent nominally to those of the numerical model in Table 1. As far as this test is concerned, its target is to modify the Z-direction dynamic behaviour of the pipeline system. Hence, the dynamic stiffness of the shock absorber (z_a) at its connection point in its axial direction, which

has a significant influence on the Z-direction vibration of the pipeline, is measured and shown in Fig. 12c. It is important to point out that such dynamic stiffness is obtained directly from a simple hammer test and does not involve any theoretical simplification of the elastic support [22]. On the other hand, the lateral dynamic stiffness of the elastic support is not required in the formulation and thus is neglected in the vibration test since they only influence the X- and Y- direction vibrations of the pipeline, not affecting the Z-direction dynamic behaviour of the pipeline system [45].

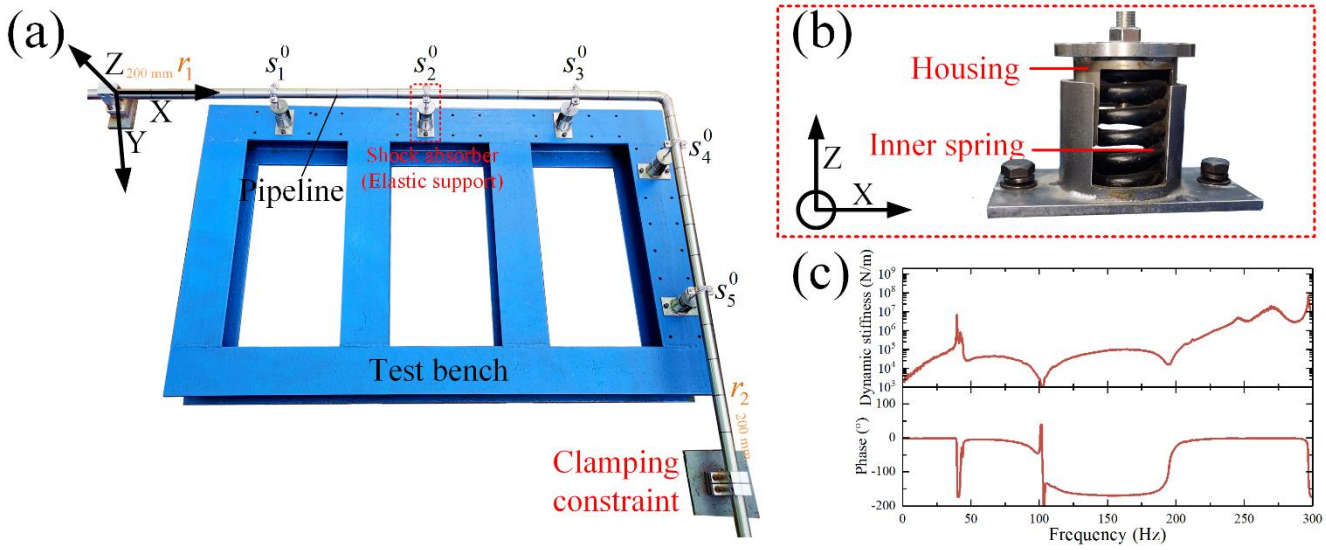

Fig. 12. Experimental setup: (a) L-shaped pipeline system; (b) elastic support; (c) dynamic stiffness parameters.

The number of measurement points affects the optimality of the elastic support layout. A higher number leads to a better capture of a mode and, thus, a more accurate representation of the FRFs of the pipeline, as reflected by Eq. (12). In order to hold on to the first four eigenstructures of the pipeline system, this work set a total of 29 measurement points along with the pipeline structure at an equal interval of 100 mm, which is the same as the numerical model in Section 3.1.

In an impact hammer test, the exciting force is imparted by an L02 Model 3A102 impact hammer with a plastic hammer tip, and the vibration responses of these measurement points are monitored through the Donghua miniature accelerometers (Model 1A116E); the force and acceleration signals involved in the test are all sampled by a DH5902 signal conditioning and data acquisition system, which passes test data to a PC in real-time. The DHDAS software

is used for signal processing and modal parameter identification.

The measured FRFs of the original pipeline system are displayed in the solid line of Fig. 13, in which the frequency range of interest is limited to a frequency below 120 Hz, which covers the first four modes of the pipeline. The modal parameters of the system are estimated through the PolyMax method [48] and shown in Fig. 14. As proof of the accuracy of modal parameters, the FRFs fitted through these modal parameters are shown in dotted lines in Fig. 13, where they are compared with those obtained from tests (solid lines).

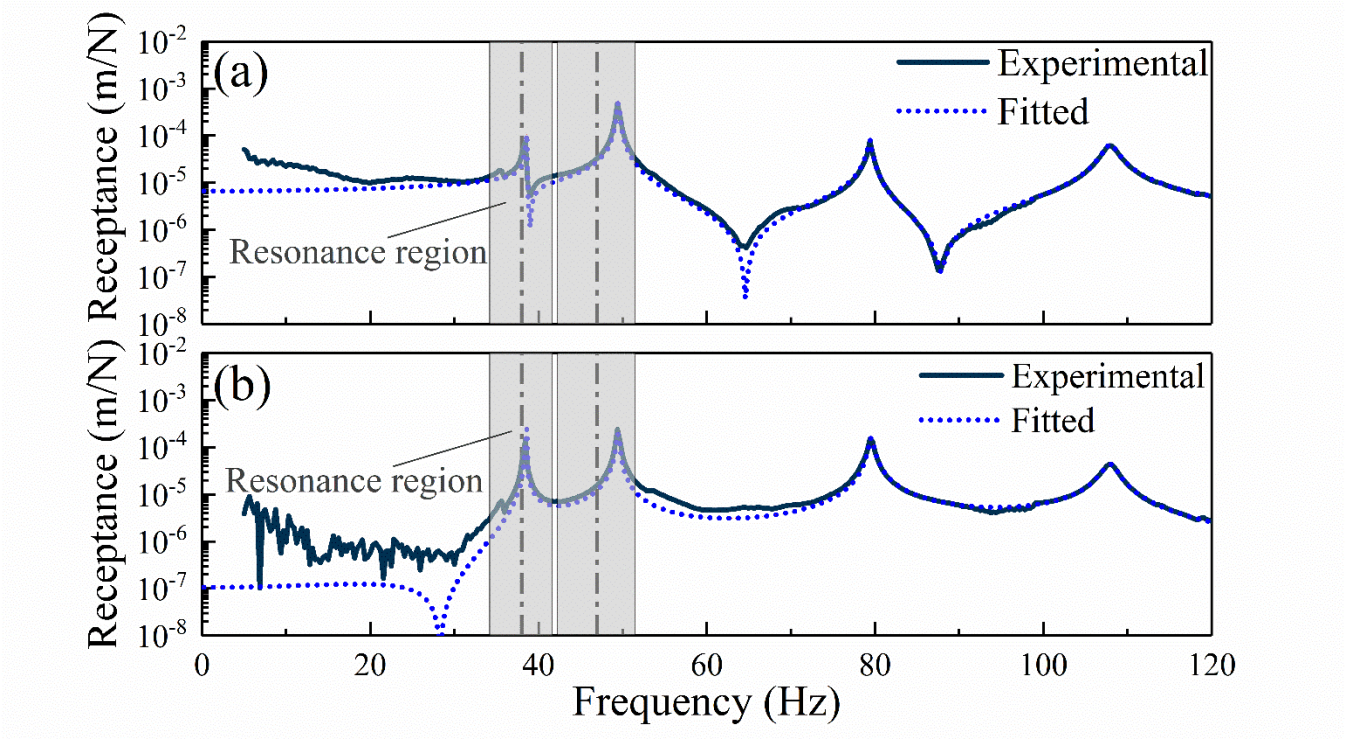

Fig. 13. Comparison between the experimental and fitted FRF: (a) $h_{s_1^0 s_1^0}$; (b) $h_{s_1^0 s_5^0}$.

When the frequencies of excitation from the power source connecting to the pipeline are within the resonance domains around 38 Hz and 47 Hz, as highlighted in shaded areas in Fig. 13, resonance happens and should be avoided. Therefore, the purpose of this work is to assign the first natural frequency of 34 Hz and the second natural frequency of 52 Hz in order to shift the first two natural frequencies out of the resonance regions.

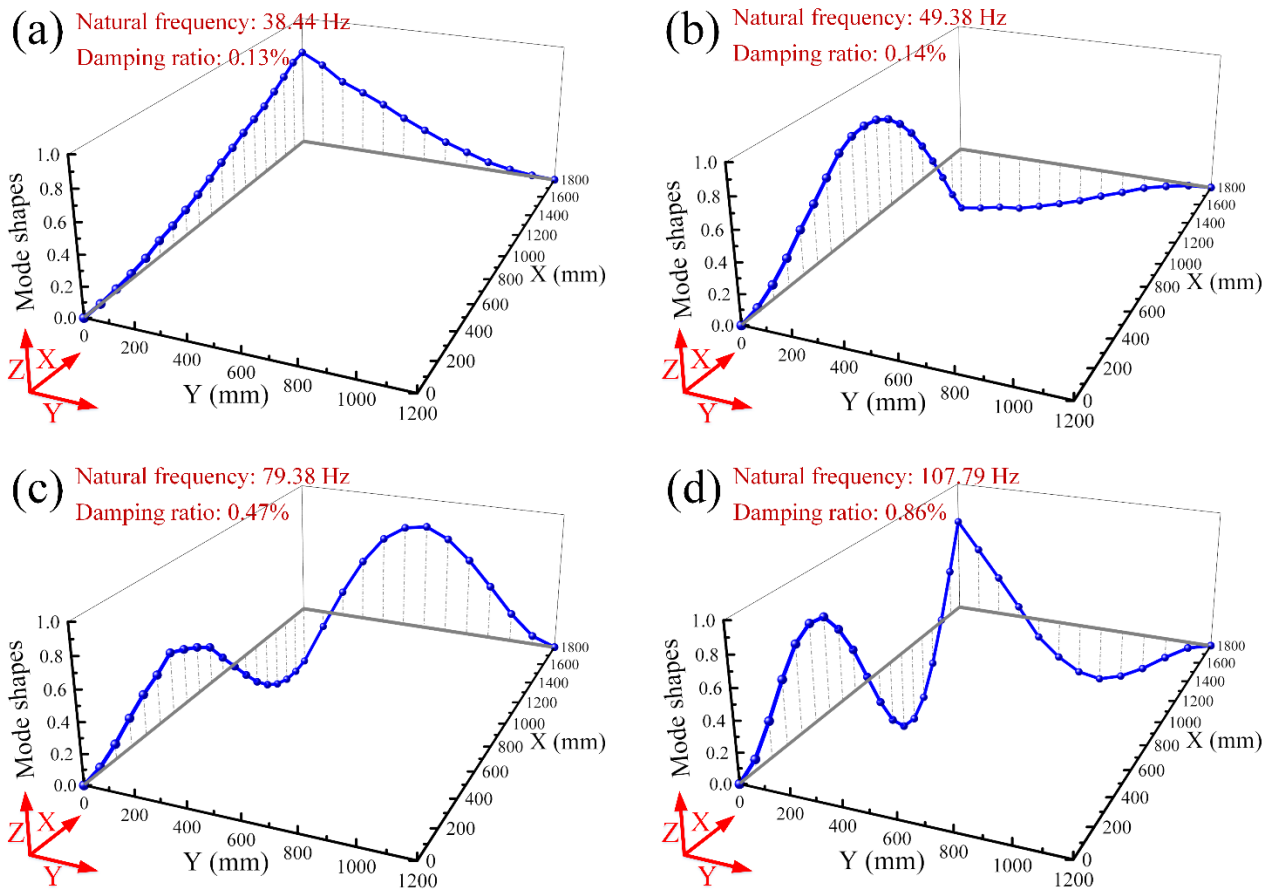

Fig. 14. First four mode shapes of the experimental pipeline system: (a) Mode 1; (b) Mode 2; (c) Mode 3; (d) Mode 4.

4.2 Natural frequency assignment of the experimental pipeline system

In this section, the proposed measurement-based layout optimization method is used to realize the aforementioned goal of natural frequency assignment physically. The relevant settings for optimization calculation are the same as in Section 3.2, and the obtained optimal locations of the elastic supports are shown in the third column of Table 7. It should be stressed that the calculation of the optimal layout of elastic supports in the present example is entirely based on the measured natural frequencies, damping ratios, and mode shape functions in Fig. 14.

The layout optimization of pipeline supports has been realized physically by moving the installation locations of elastic supports, which allows the closest approximation of the calculated optimal layout. The experimental pipeline system after layout optimization is shown in Fig. 15.

Table 7. Initial and optimal locations of elastic supports for the experimental pipeline system.

Location	Initial $(x_{s_i^0}, y_{s_i^0})$	Optimal $(x_{s_i^0+\Delta s_i}, y_{s_i^0+\Delta s_i})$	Realized (x_{s_i}, y_{s_i})
s_1 (mm)	(500, 0)	(500+196.4, 0)	(700.0, 0)
s_2 (mm)	(1000, 0)	(1000-87.8, 0)	(900.0, 0)
s_3 (mm)	(1500, 0)	(1500-204.4, 0)	(1300.0, 0)
s_4 (mm)	(1800, 200)	(1800, 200+142.1)	(1800, 350)
s_5 (mm)	(1800, 700)	(1800, 700-119.4)	(1800, 600)

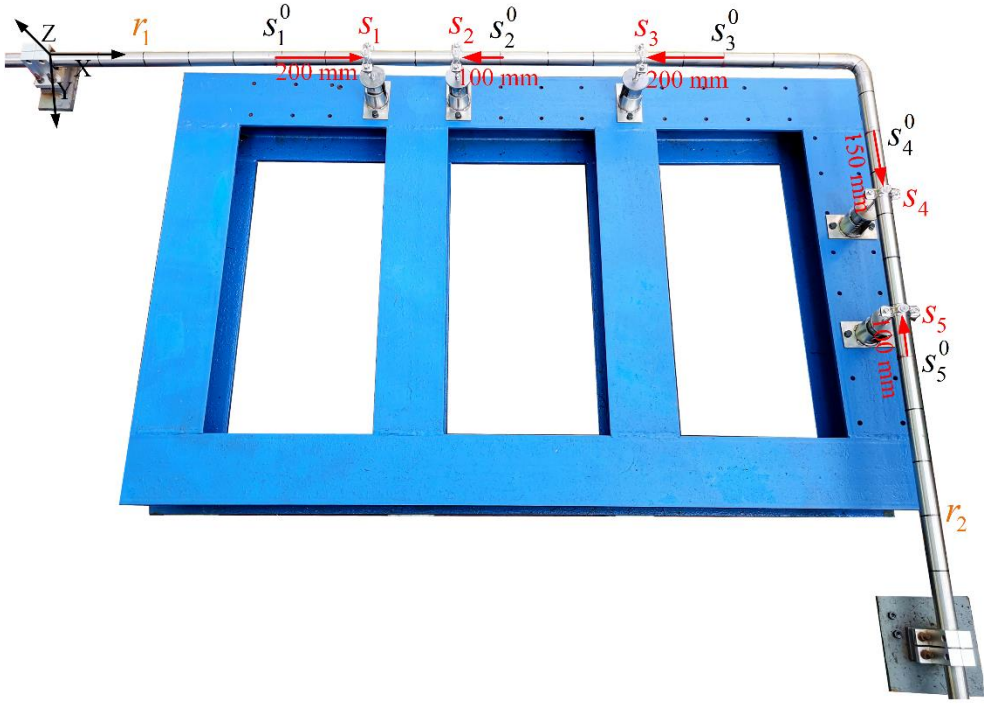

Fig. 15. Experimental pipeline system with the optimal layout of elastic supports.

The same test equipment and procedure described in Section 4.1 have been used for the FRF measurement of the modified pipeline system. The measured FRFs ($h_{s_1 s_1}$ and $h_{s_1 s_5}$) are displayed in Fig. 16, from which the first two natural frequencies of the modified system are identified and collected in Table 8.

Clearly, Fig. 16 and Table 8 reveal that the natural frequencies of the experimental pipeline system after layout optimization match almost perfectly the target ones. Only small errors in the assigned natural frequencies can be observed, which is partly because of the approximate implementation of the support locations to the theoretical ones.

As a piece of experimental evidence, such a result gives the confidence to employ the proposed method to solve the resonance problem of pipeline systems in practice.

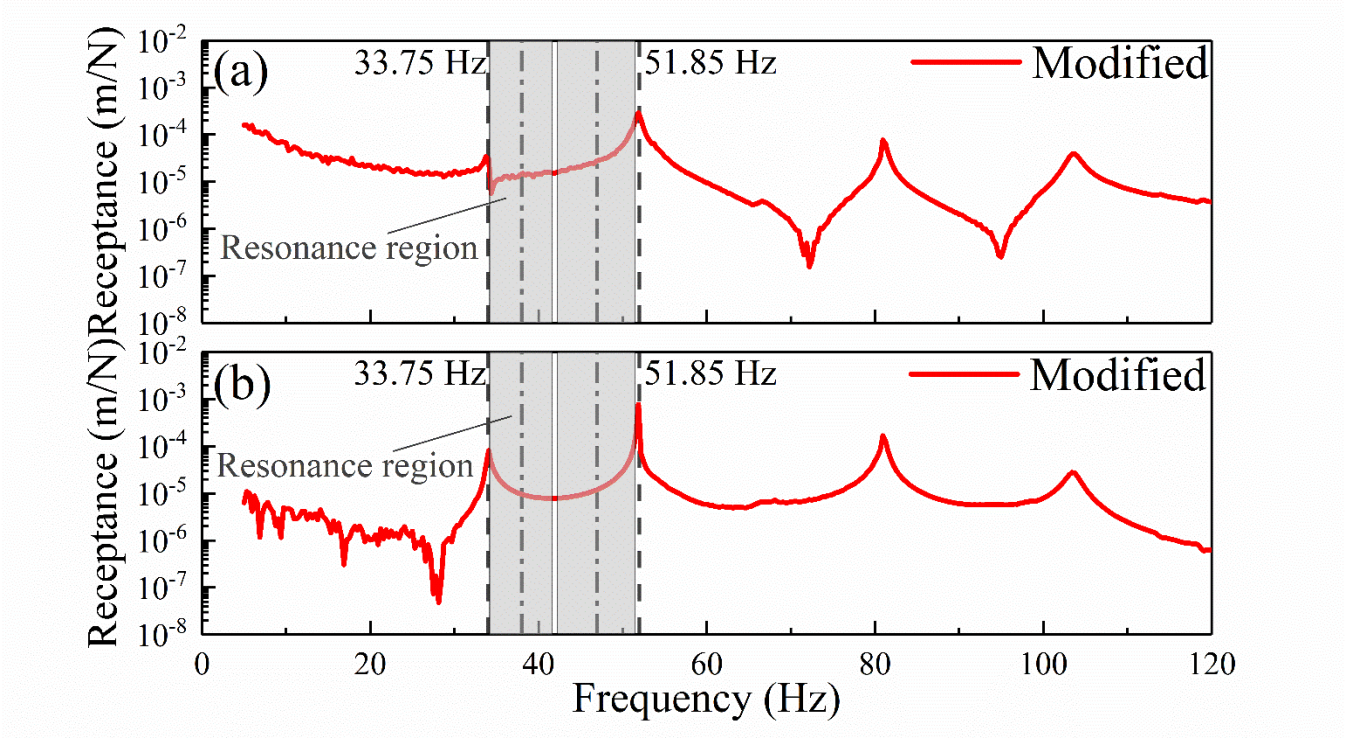

Fig. 16. FRFs of the experimental pipeline system after layout optimization: (a) $h_{s_1 s_1}$; (b) $h_{s_1 s_5}$.

Table 8. First four natural frequencies of the experimental pipeline system after layout optimization.

	Natural frequency	Target frequency	Error	Whether in resonance
Mode 1	33.75 Hz	34.00 Hz	-0.74%	No
Mode 2	51.85 Hz	52.00 Hz	-0.29%	No
Mode 3	80.94 Hz	-	-	No
Mode 4	103.44 Hz	-	-	No

Finally, a forced vibration test of the pipeline is carried out to assess the vibration suppression performance of the proposed method. A harmonic excitation force in the Z-direction is applied to the measurement point r_1 by using a vibration exciter, and the vibration response in the Z-direction of the measurement point r_2 is measured through an accelerometer. The location coordinates of measuring points r_1 and r_2 are shown in Fig. 12. The magnitude of

the excitation force is 10 N, and the frequency of excitation is respectively 38 Hz and 47 Hz, which correspond to the central frequency of the two resonance regions in Fig. 16.

The vibration responses of location r_2 before and after layout optimization at the two frequencies of excitation are shown in Fig. 17, and the corresponding vibration amplitudes are identified and collected in Table 9. It can be seen from Fig. 17 and Table 9 that the vibration of location r_2 after the optimized support layout decreases obviously at the two frequencies of excitation, with a reduction ratio of more than 50%. Such a result corroborates the effectiveness of the proposed layout optimization method in suppressing vibration and solving the resonance problem of a post-manufactured pipeline.

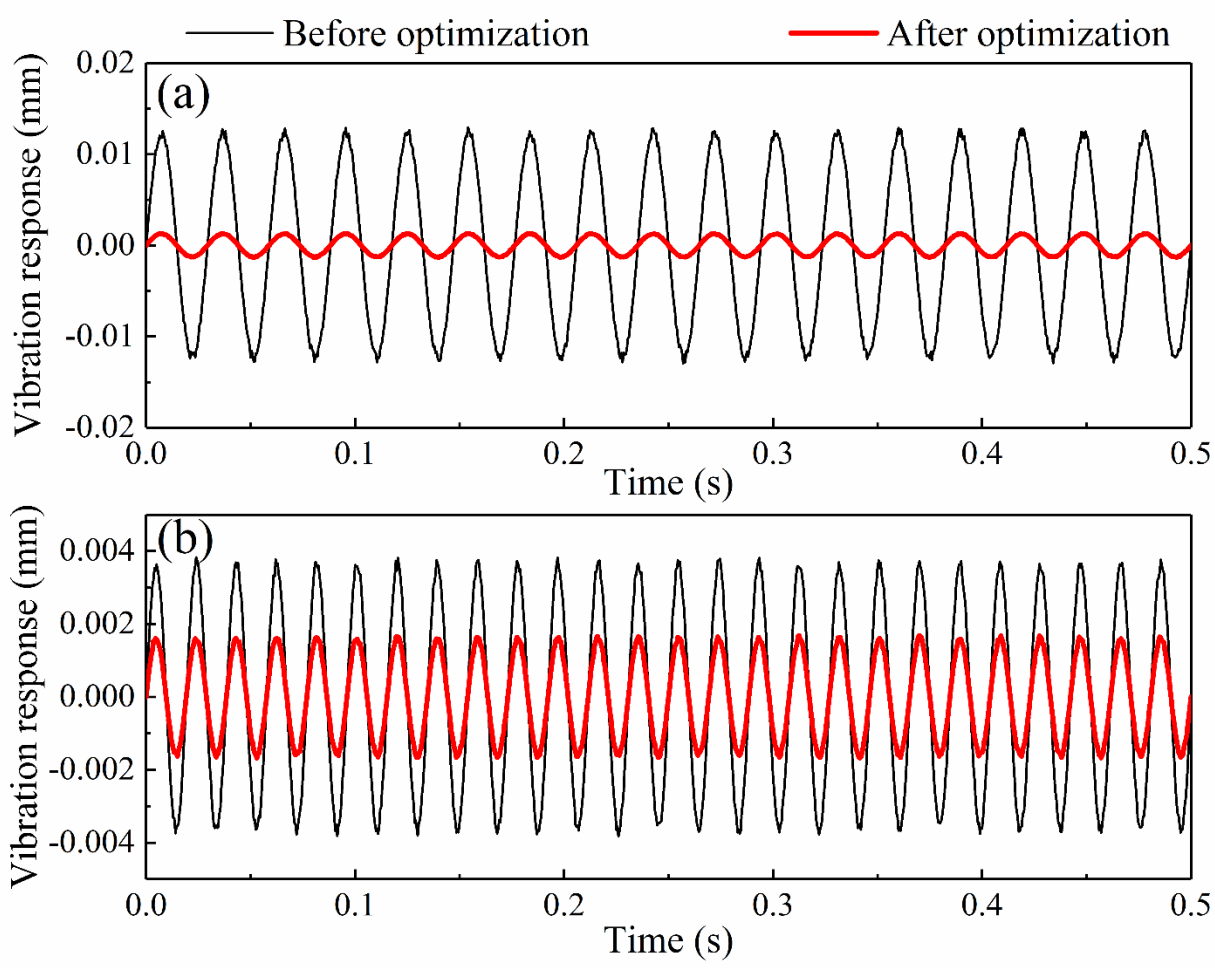

Fig. 17. Vibration response of measurement point r_2 under harmonic excitation before and after layout optimization: (a) excitation frequency is 38 Hz; (b) excitation frequency 47 Hz.

Table 9 Vibration amplitude of measurement point r_2 before and after layout optimization

	Before optimization	After optimization	Reduction
Excitation frequency 38 Hz	0.01233 mm	0.00132 mm	89.29%
Excitation frequency 47 Hz	0.00378 mm	0.00168 mm	55.56%

5. Conclusions

This paper reports the first theoretical and experimental study that concerns only using the measured data to realize the layout optimization of pipeline support for addressing the resonance problem of the industrial post-manufactured pipeline system. Such a study recasts the resonance avoidance problem of pipeline systems as a structural modification problem for natural frequency assignment. The optimal locations of pipeline supports are obtained through the measurement-based layout optimization method of pipeline elastic supports proposed in this paper. In this method, the measured dynamic stiffness parameters can be directly used to describe the dynamic behavior of elastic supports, and thus it is unnecessary to prescribe the simplified form of the elastic support. The determination of the optimal locations does not involve the theoretical or numerical model of the pipeline system, requiring only measured modal parameters. This proposed method can help to tackle the resonance problem of the post-manufactured pipeline system in practice.

In this work, the proposed method achieves the layout optimization of pipeline elastic supports by carrying out structural modification in two stages. The target of the first stage of structural modification is used for preprocessing measured modal parameters of the original pipeline system and estimating the eigenstructure of the pipeline without elastic supports. The second stage of structural modification aims to find the optimal locations of these elastic supports and realize their layout optimization. In this stage, the basic framework of the receptance method is employed, and the assignment problem of natural frequencies is expressed as a nonlinear equation about the unknown optimal locations, which can be easily solved by utilizing a global optimization algorithm. The effectiveness of the proposed method is demonstrated by a series of examples, including numerical and experimental cases.

Finally, some limitations of the proposed method should be highlighted: NSGA-II algorithm employed in this work

has good performance when solving low-dimensional optimization problems (the number of target frequencies and elastic supports is relatively small); however, it may have the problems of slow convergence or stagnation when dealing with high dimensional optimization problems (the number of target frequencies >6 or the number of elastic supports >20). Therefore, it is suggested to replace the NSGA-II algorithm with the high-dimensional multiobjective optimization algorithm to solve the established objective function of natural frequency assignment when employing the proposed method to deal with a high-dimensional layout optimization problem of pipeline supports.

Author Contributions

Lin Zhang: Conceptualization, Methodology, Validation, Software, Formal analysis, Writing - original draft, Visualization. **Tao Zhang:** Conceptualization, Investigation, Resources, Supervision, Software, Funding acquisition, Writing - review & editing. **Huajiang Ouyang:** Methodology, Formal analysis, Validation, Formal analysis, Investigation, Writing - review & editing, Project administration. **Tianyun Li:** Conceptualization, Validation, Formal analysis, Investigation, Funding acquisition, Data curation, Project administration. **Mo You:** Software, Validation, Visualization

Acknowledgments

This research was funded by the National Natural Science Foundation of China, grant numbers 10702022 and 51839005.

Conflict of interest

We declare that we have no commercial or associative interest that represents a conflict of interest connected with the work submitted

References

[1] J. Łuczko, A. Czerwiński, Three-dimensional dynamics of curved pipes conveying fluid. Journal of Fluids and Structures, 91 (2019) 102704.

[2] L. Maxit, M. Karimi, O. Guasch, Spatial coherence of pipe vibrations induced by an internal turbulent flow. Journal of Sound and Vibration, 493 (2021) 115841.

[3] J.M. Muggleton, M. Kalkowski, Y. Gao, E. Rustighi, A theoretical study of the fundamental torsional wave in buried pipes for pipeline condition assessment and monitoring. Journal of Sound and Vibration, 374 (2016) 155-171.

[4] S. Li, M. Han, Z. Cheng, C. Xia, Multi-modal identification of leakage-induced acoustic vibration in gas-filled pipelines by selection of coherent frequency band. International Journal of Pressure Vessels and Piping, 188 (2020) 104193.

[5] B.A. Khudayarov, K.M. Komilova, F.Z. Turaev, J.A. Aliyarov, Numerical simulation of vibration of composite pipelines conveying fluids with account for lumped masses. International Journal of Pressure Vessels and Piping, 179 (2020) 104034.

[6] X. Guo, H. Ge, C. Xiao, H. Ma, W. Sun, H. Li, Vibration transmission characteristics analysis of the parallel fluid-conveying pipes system: Numerical and experimental studies. Mechanical Systems and Signal Processing, 177 (2022) 109180.

[7] Q. Ni, Y. Luo, M. Li, H. Yan, Natural frequency and stability analysis of a pipe conveying fluid with axially moving supports immersed in fluid. Journal of Sound and Vibration, 403 (2017) 173-189.

[8] J. Łuczko, A. Czerwiński, Experimental and numerical investigation of parametric resonance of flexible hose conveying non-harmonic fluid flow. Journal of Sound and Vibration, 373 (2016) 236-250.

[9] D. Yano, S. Ishikawa, K. Tanaka, S. Kijimoto, Vibration analysis of viscoelastic damping material attached to a cylindrical pipe by added mass and added damping. Journal of Sound and Vibration, 454 (2019) 14-31.

[10] X. Tan, X. Mao, H. Ding, L. Chen, Vibration around non-trivial equilibrium of a supercritical Timoshenko pipe conveying fluid. Journal of Sound and Vibration, 428 (2018) 104-118.

[11] Y. Yang, Z. Qin, Y. Zhang, Random response analysis of hydraulic pipeline systems under fluid fluctuation and base motion. Mechanical Systems and Signal Processing, 186 (2023) 109905.

[12] L. Zhang, T. Zhang, H. Ouyang, T. Li, S. Zhang, Receptance-based natural frequency assignment of a real fluid-conveying pipeline system with interval uncertainty. Mechanical Systems and Signal Processing, 179 (2) (2022) 109321.

[13] Y. Lin, R. Huang, C. Chu, Optimal modal vibration suppression of a fluid-conveying pipe with a divergent mode. Journal of Sound and Vibration, 271 (3-5) (2004) 577-597.

[14] D. Wang, M. Wen, Vibration attenuation of beam structure with intermediate support under harmonic excitation. Journal of Sound and Vibration, 532 (2022) 117008.

[15] A. Kwong, K. Edge, A method to reduce noise in hydraulic systems by optimizing pipe clamp locations. Proceedings of the Institution of Mechanical Engineers. Part I, Journal of Systems and Control engineering, 212 (4) (1998) 267-280.

[16] J. Herrmann, T. Haag, L. Gaul, Experimental and numerical investigation of the dynamics in spatial fluid-filled piping systems. The Journal of the Acoustical Society of America, 123 (5) (2008) 3422.

[17] Z. Tang, Z. Lu, D. Li, F. Zhang, Optimal design of the positions of the hoops for a hydraulic pipelines system. Nuclear Engineering and Design, 241 (12) (2011) 4840-4855.

[18] P. Gao, J. Li, J. Zhai, Y. Tao, Q. Han, A novel optimization layout method for clamps in a pipeline system. Applied Sciences, 10 (1) (2020) 390.

[19] X. Li, W. Li, J. Shi, Q. Li, S. Wang, Pipelines vibration analysis and control based on clamps' locations optimization of multi-pump system. Chinese Journal of Aeronautics, 35 (6) (2022) 352-366.

[20] Y. Huang, Y. Liu, B. Li, Y. Li, Z. Yue, Natural frequency analysis of fluid conveying pipeline with different boundary conditions. Nuclear Engineering and Design, 240 (3) (2010) 461-467.

[21] D. Wang, W. Sun, Z. Gao, H. Ma, Optimization of spatial pipeline with multi-hoop supports for avoiding resonance problem based on genetic algorithm. Science Progress, 105 (1) (2022) 39829264.
[22] T. Zhang, H. Ouyang, C. Zhao, Y.J. Ding, Vibration analysis of a complex fluid-conveying piping system with general boundary conditions using the receptance method. International Journal of Pressure Vessels and Piping, 166 (2018) 84-93.
[23] P. Gao, T. Yu, Y. Zhang, J. Wang, J. Zhai, Vibration analysis and control technologies of hydraulic pipeline system in aircraft: A review. Chinese Journal of Aeronautics, 34 (4) (2021) 83-114.
[24] R. Belotti, D. Richiedei, Dynamic structural modification of vibrating systems oriented to eigenstructure assignment through active control: A concurrent approach. Journal of Sound and Vibration, 422 (2018) 358-372.
[25] Z. Wang, S. Lei, L. Cheng, Y. Yang, L. Ding, Response prediction for mechanical systems subject to combinational structural modifications. Journal of Sound and Vibration, 534 (2022) 117019.
[26] L. Zhang, T. Zhang, H. Ouyang, T. Li, Receptance-based antiresonant frequency assignment of an uncertain dynamic system using interval multiobjective optimization method. Journal of Sound and Vibration, 529 (10) (2022) 116944.
[27] Z. Liu, W. Li, H. Ouyang, D. Wang, Eigenstructure assignment in vibrating systems based on receptances. Archive of Applied Mechanics, 85 (6) (2015) 713-724.
[28] J.E. Mottershead, Y.M. Ram, Inverse eigenvalue problems in vibration absorption: Passive modification and active control. Mechanical Systems and Signal Processing, 20 (1) (2006) 5-44.
[29] O. Cakar, Mass and stiffness modifications without changing any specified natural frequency of a structure. Journal of Vibration and Control, 17 (5) (2010) 769-776.
[30] H. Ouyang, D. Richiedei, A. Trevisani, G. Zanardo, Eigenstructure assignment in undamped vibrating systems：A convex-constrained modification method based on receptances. Mechanical Systems and Signal Processing, 27 (1) (2012) 397-409.
[31] H. Ouyang, D. Richiedei, A. Trevisani, G. Zanardo, Discrete mass and stiffness modifications for the inverse eigenstructure assignment in vibrating systems: Theory and experimental validation. International Journal of Mechanical Sciences, 64 (1) (2012) 211-220.
[32] H. Liu, H. Gao, Y. Ma, Receptance-based assignment of dynamic characteristics: A summary and an extension. Mechanical Systems and Signal Processing, 145 (2020) 106913.
[33] D. Richiedei, I. Tamellin, A. Trevisani, Pole-zero assignment by the receptance method: multi-input active vibration control. Mechanical Systems and Signal Processing, 172 (2022) 108976.
[34] J.E. Mottershead, M. Ghandchi Tehrani, D. Stancioiu, S. James, H. Shahverdi, Structural modification of a helicopter tailcone. Journal of Sound and Vibration, 298 (1-2) (2006) 366-384.
[35] R. Caracciolo, D. Richiedei, A. Trevisani, G. Zanardo, Designing vibratory linear feeders through an inverse dynamic structural modification approach. The International Journal of Advanced Manufacturing Technology, 80 (9-12) (2015) 1587-1599.
[36] O. Zarraga, I. Ulacia, J.M. Abete, H. Ouyang, Receptance based structural modification in a simple brake-clutch model for squeal noise suppression. Mechanical Systems and Signal Processing, 90 (2017) 222-233.
[37] S. Tsai, H. Ouyang, J. Chang, Inverse structural modifications of a geared rotor-bearing system for frequency assignment using measured receptances. Mechanical Systems and Signal Processing, 110 (2018) 59-72.
[38] D. Richiedei, I. Tamellin, A. Trevisani, Simultaneous assignment of resonances and antiresonances in vibrating systems through inverse dynamic structural modification. Journal of Sound and Vibration, 485 (2020) 115552.
[39] D. Wang, M.I. Friswell, Support position optimization with minimum stiffness for plate structures including support mass. Journal of Sound and Vibration, 499 (2021) 116003.
[40] B. Yan, M.J. Brennan, S.J. Elliott, N.S. Ferguson, Characteristics of distributed parameter isolators. Journal of Sound and Vibration, 320 (3) (2009) 516-526.
[41] X. Zhang, W. Liu, Y. Zhang, Y. Zhao, Experimental investigation and optimization design of multi-support pipeline system. Chinese Journal of Mechanical Engineering, 34 (10) (2021) 33-53.

[42] Y. Shi, S. Li, An inverse modification method for assigning antiresonant frequencies. Applied Acoustics, 170 (2020) 107524.
[43] S. Cong, S.J. Hu, H. Li, FRF-based pole-zero method for finite element model updating. Mechanical Systems and Signal Processing, 177 (2022) 109206.
[44] S. Tsai, H. Ouyang, J. Chang, Identification of torsional receptances. Mechanical Systems and Signal Processing, 126 (2019) 116-136.
[45] X. Guo, Y. Cao, H. Ma, C. Xiao, B. Wen, Dynamic analysis of an L-shaped liquid-filled pipe with interval uncertainty. International Journal of Mechanical Sciences, 217 (2022) 107040.
[46] D. Richiedei, I. Tamellin, Active approaches to vibration absorption through antiresonance assignment: A comparative study. Applied Sciences, 11 (3) (2021) 1091.
[47] K. Deb, A. Pratap, S. Agarwal, T. Meyarivan, A fast and elitist multiobjective genetic algorithm: NSGA-II. IEEE Transactions on Evolutionary Computation, 6 (2) (2002) 182-197.
[48] B. Peeters, H. Van Der Auweraer, P. Guillaume, J. Leuridan, The PolyMAX frequency-domain method: a new standard for modal parameter estimation? Shock and Vibration, 11 (3-4) (2004) 395-409.